EUR 2734.e

EUROPEAN ATOMIC ENERGY COMMUNITY - EURATOM

HYDROGEN MOTION IN PRIMARY SOLUTIONS OF HYDROGEN IN SOME TRANSITION ELEMENTS

by

W. KLEY, J. PERETTI, R. RUBIN and G. VERDAN

1966

Joint Nuclear Research Center
Ispra Establishment - Italy

Reactor Physics Department
Experimental Neutron Physics

Paper presented at the
BROOKHAVEN National Laboratory Symposium
Upton, L.I., N.Y., USA - September 20-22, 1965

This report is on sale at the addresses listed on cover page 4.

at the price of	FF 7,—	FB 70,—	DM 5.60	Lit. 870	Fl. 5.10

When ordering, please quote the EUR number and the title, which are indicated on the cover of each report.

Printed by Smeets s.a.
Brussel, February 1966

EUR 2734.e

HYDROGEN MOTION IN PRIMARY SOLUTIONS OF HYDROGEN IN SOME TRANSITION ELEMENTS by W. KLEY, J. PERETTI, R. RUBIN and G. VERDAN

European Atomic Energy Community - EURATOM
Joint Nuclear Research Center - Ispra Establishment (Italy)
Reactor Physics Department - Experimental Neutron Physics
Paper presented at the Brookhaven National Laboratory Symposium
Upton, L.I., N.Y., USA - September 20-22, 1965
Brussels, February 1966 - 52 Pages - 14 Figures - FB 70

The scattering of cold neutrons was measured from VH_x, NbH_x and PdH_x systems at low hydrogen concentrations. The difference of the

EUR 2734.e

HYDROGEN MOTION IN PRIMARY SOLUTIONS OF HYDROGEN IN SOME TRANSITION ELEMENTS by W. KLEY, J. PERETTI, R. RUBIN and G. VERDAN

European Atomic Energy Community - EURATOM
Joint Nuclear Research Center - Ispra Establishment (Italy)
Reactor Physics Department - Experimental Neutron Physics
Paper presented at the Brookhaven National Laboratory Symposium
Upton, L.I., N.Y., USA - September 20-22, 1965
Brussels, February 1966 - 52 Pages - 14 Figures - FB 70

The scattering of cold neutrons was measured from VH_x, NbH_x and PdH_x systems at low hydrogen concentrations. The difference of the

EUR 2734.e

HYDROGEN MOTION IN PRIMARY SOLUTIONS OF HYDROGEN IN SOME TRANSITION ELEMENTS by W. KLEY, J. PERETTI, R. RUBIN and G. VERDAN

European Atomic Energy Community - EURATOM
Joint Nuclear Research Center - Ispra Establishment (Italy)
Reactor Physics Department - Experimental Neutron Physics
Paper presented at the Brookhaven National Laboratory Symposium
Upton, L.I., N.Y., USA - September 20-22, 1965
Brussels, February 1966 - 52 Pages - 14 Figures - FB 70

The scattering of cold neutrons was measured from VH_x, NbH_x and PdH_x systems at low hydrogen concentrations. The difference of the

normalized intensities of the «hydrogen system» and the pure host lattice, reveals the neutron scattering distribution of the «hydrogen probe» in the host lattice. Those intensity distributions show the expected high energy «Local modes» of the hydrogen impurity well above the maximum frequency of the host lattice. For VH_x and NbH_x in the α phase, also a low energy neutron distribution of a few meV is observed, close to the energy of the impinging neutrons. Apart of a certain distortion near the maximum host lattice frequency, in addition, the host lattice frequency distribution can be « seen » through the hydrogen « Band modes ». For Nb, two pronounced peaks are found at energy transfers of 25,9 and 18,3 meV. They agree reasonably well with recent calculations of the frequency distribution of Nb.

normalized intensities of the «hydrogen system» and the pure host lattice, reveals the neutron scattering distribution of the «hydrogen probe» in the host lattice. Those intensity distributions show the expected high energy «Local modes» of the hydrogen impurity well above the maximum frequency of the host lattice. For VH_x and NbH_x in the α phase, also a low energy neutron distribution of a few meV is observed, close to the energy of the impinging neutrons. Apart of a certain distortion near the maximum host lattice frequency, in addition, the host lattice frequency distribution can be « seen » through the hydrogen « Band modes ». For Nb, two pronounced peaks are found at energy transfers of 25,9 and 18,3 meV. They agree reasonably well with recent calculations of the frequency distribution of Nb.

normalized intensities of the «hydrogen system» and the pure host lattice, reveals the neutron scattering distribution of the «hydrogen probe» in the host lattice. Those intensity distributions show the expected high energy «Local modes» of the hydrogen impurity well above the maximum frequency of the host lattice. For VH_x and NbH_x in the α phase, also a low energy neutron distribution of a few meV is observed, close to the energy of the impinging neutrons. Apart of a certain distortion near the maximum host lattice frequency, in addition, the host lattice frequency distribution can be « seen » through the hydrogen « Band modes ». For Nb, two pronounced peaks are found at energy transfers of 25,9 and 18,3 meV. They agree reasonably well with recent calculations of the frequency distribution of Nb.

EUR 2734.e

EUROPEAN ATOMIC ENERGY COMMUNITY - EURATOM

HYDROGEN MOTION IN PRIMARY SOLUTIONS OF HYDROGEN IN SOME TRANSITION ELEMENTS

by

W. KLEY, J. PERETTI, R. RUBIN and G. VERDAN

1966

Joint Nuclear Research Center
Ispra Establishment - Italy

Reactor Physics Department
Experimental Neutron Physics

Paper presented at the
BROOKHAVEN National Laboratory Symposium
Upton, L.I., N.Y., USA - September 20-22, 1965

Summary

The scattering of cold neutrons was measured from VH_x, NbH_x and PdH_x systems at low hydrogen concentrations. The difference of the normalized intensities of the «hydrogen system» and the pure host lattice, reveals the neutron scattering distribution of the «hydrogen probe» in the host lattice. Those intensity distributions show the expected high energy «Local modes» of the hydrogen impurity well above the maximum frequency of the host lattice. For VH_x and NbH_x in the α phase, also a low energy neutron distribution of a few meV is observed, close to the energy of the impinging neutrons. Apart of a certain distortion near the maximum host lattice frequency, in addition, the host lattice frequency distribution can be « seen » through the hydrogen « Band modes ». For Nb, two pronounced peaks are fouad at energy transfers of 25,9 and 18,3 meV. They agree reasonably well with recent calculations of the frequency distribution of Nb.

Content

---

1. Introduction (°)

The problems connected with impurities have gained a great interest in recent years particularly in connection with the studies of semi-conductors, color centers, diffusion process in solids and the Mössbauer effect. Many physical phenomena are more strongly dependent on the concentration of impurities than on the host itself. This behaviour of crystals with impurities gives a great importance to the study of the eigen-vibrations of the impurity in the solid. As it is established in a well known series of papers [1-6], the introduction of an impurity atom into an ideal crystal causes a modification of the normal modes. Under certain conditions "Local" and "Band" modes of the impurity atom are appearing. A particular clear discussion of this phenomena is given by Dawber and Elliott [7] and Kagan and Josilevskii [8]. The existance of "Local Modes" was experimentally well established by Infrared [9] and Raman [10] Spectrometry. By the inelastic scattering of neutrons Mozer et al. [11] and Rubin et al. [12] have brought evidence of local modes in solid solutions.

In the interaction of neutrons with impurities it is most important to know the cross section since otherwise only very qualitative arguments can be used for the interpreation of the data. The best approach for calculating the cross section for an impurity is actually given in the paper by Zemach and Glauber [13] and in the very general and most complete work by Kagan and Josilevskii [8]. In this paper we deal primarily with an impurity that scatters the neutrons almost entirely incoherently, therefore we can make use of a simplified procedure using the Zemach and Glauber formalism. One of the central questions is still what kind of information can be obtained by the inelastic scattering of cold neutrons ? The "Local modes" can be visualized but they will not reveal details about the host itself.

(°) Manuscript received on January 7, 1965

With the measurements of the band modes the eigen-frequency distribution of the host lattice can be obtained. Difference measurements of the crystal with impurity and the pure crystal will reveal all the motions of the impurity atom in the lattice. We have choosen to study hydrogen in some transition elements because of the general interest in solid solutions of hydrogen and particular of being best suited for neutron measurements since it has a very large incoherent scattering cross section. Therefore no coherence distruction will influence the shape of the difference of the neutron distribution of the impure and pure crystal independent if the host atoms will have coherent or incoherent cross section. Hence the difference measurements will reveal the hydrogen vibration in the host lattice without any distortion.

Hydrogen in transition metals is soluable up to a certain concentration with only very small changes in the host lattice; this range is called the α-phase, the physical status of the solid solution and with increasing concentration the β-Hydride phase is formed. Since we are primarily interested in the behaviour of an impurity in a host lattice then instead of a compound like substance, our measurements were carried out in the α-phase, the solid solution state. The different physical status of the α-and β-phase cannot be seen only by the change of the crystal structure but also by the different heat of solution, f.i., of hydrogen in Nb; the heat of solution increases from 16.1 kcal/mole at H/Nb = 0.01 to 23.3 kcal/mole at H/Nb = 0.70, the β-phase. For Vanadium the phase diagram, Fig. [1], is rather well known and therefore a sequence of measurements were made with the VH0.09 at various temperatures. The data are given in Fig. [2], they reveal the effect of the phase transition from the two phases (α+β) to the pure α-phase. The β-phase has an optical peak at an energy of E $\approx$ 60 meV while the "Local" mode of the α-phase is peaking at $E_n \approx 100$ meV. In this paper, emphasize is given to measurements of Hydrogen in solid solution.

2. Experimental Methods

The samples were prepared by using standard methods for hydration. All the sample were heated up to 800°C in a high vacuum apparatus for purifying the samples from Oxygen and Nitrogen as well as Hydrogen itself. After a sufficient long time of purification the samples were put under a pressure of spectroscopically pure Hydrogen at a temperature of 800°C. The final hydration was made at 400°C and towards room temperature. The hydrogen content was measured volumetrically and by weighing the samples before and after hydration. Satisfactory agreement was obtained for both methods.

The neutron measurements were carried out using the Ispra-I cold neutron facility [14]. The measurements concerning the phase transition in Fig. [2] were carried out by using a flight path of 5.5 meter. All the other measurements were made using a 3 meter flight path. The energy resolution was sufficient with 3 meter since the "Local excitations" have a natural width that is many times larger than the resolution width. All the data in this paper have been corrected for : 1) Background, 2) Sample thickness, 3) Air attenuation in the flight path, and 4) The counter efficiency. For a number of samples and measurements, the data were converted and the generalized frequency distribution function G(E) presented. For the convertion from the time to the energy scale, the experimental points were fitted to a smooth curve in order to minimize the experimental error of each particular point. The smooth curves in the energy scale are marked at a few energy points with the experimental errors involved. The generalized frequency distribution function is defined in equation (8) and given by :

$$G(E) = \frac{d^2\mathcal{J}}{d\Omega\, dE} * \frac{1}{\mathcal{F}(E)} = \frac{d^2\mathcal{J}}{d\Omega\, dE} * \frac{8\pi\, k_i * E * (e^{\frac{E}{T}} - 1)}{k_f * \vec{K}^2}$$

3. The Experimental Results

3.1. The VH_n - Data

In Fig.3, the difference of the inelastically scattered neutron intensity distribution of $VH_{0.04}$ and V is plotted. This data reveals in detail the motion of the hydrogen in the Vanadium lattice. There is a very broad band of "Local" modes but also the "Band" or collective modes have contributed to the neutron intensity in the frequency range of the host lattice. In addition, the "elastically" scattered neutrons have been observed, shown in detail in Fig.12; quite a large intensity contribution can be attributed either to neutrons suffering a very small energy transfer by inelastic scattering or to a quasi elastic scattering process. The experimental results may be understood in terms of two quite different models :

I. The Lattice Dynamics of Impurities in Metals

II. A Proton Band Theory.

The accuracy of the present day data does not allow to distinguish between those two models that give a quite different "picture" of the proton-motion in the Vanadium lattice. Very high energy resolution experiments ($\frac{\Delta E}{E} \approx 2\%$) are being carried out to clarify this point. A shape analysis of the quasi elastic scattered neutrons is necessary for a possible distinction on the two models. In the following we discuss our results in view of the two models :

I. The Lattice Dynamics of Impurities in Metals

The problem of the normal modes in a crystal containing an isolate impurity was treated in its very general form in a known series of papers [1 to 6]. In these papers, it is predicted, that "Local" and "Band" modes should appear in the eigen-frequency distribution of the impurity.

Therefore, it can be understood qualitatively, that the intensity distribution of the inelastically scattered neutrons reveal such "Local" and "Band" motions of the proton in the Vanadium host lattice. However, on the basis of these general theories, one would not expect a "quasi elastic" scattering of cold neutrons as it is observed in our measurements. For this reason, we follow a suggestion of Kazarnovskii and Stepanov [15] by introducing a finite life time for the "Local" modes, that could cause a quasi elastic contribution of the scattered neutrons. This is not unreasonable, particular in view of recent measurements of Mirlin and Reshina [16] on the temperature dependence of the infrared absorption line width due to local vibrations of H^- and D^- in K·Cl and K·Br. At room temperature, a line width of about 5 meV was found. Such a line width corresponds to a life time of the order of 10^{-12} sec. If the local modes of the protons in Vanadium have similar life times, than they can cause a quasi elastic peak of the type observed in our measurements.

From the work of Dawber and Elliott [7] we know that the amplitude of the impurity atom is decreasing with increasing frequency in the host lattice frequency range. Both effects, the quasi elastic scattering and the amplitude dependence of the impurity in the "Band" mode region, can be investigated in the VH_n system. For that, we have to examine in more detail the quantitative contributions of the host lattice and the impurity atoms to the scattered neutron intensity. A general treatment of this problem including the contributions of "Local" and "Band" modes was given by Yu. Kagan and Ya. Josilevskii already in 1963. For simplicity, we use for our particular problem of a Hydrogen impurity that has an almost entirely incoherent scattering cross section, the formalism, as derived by Zemach and Glauber [13].

The partial differential cross section is given by :

$$(1)\quad \frac{d^2\sigma}{d\Omega\, dE} = \frac{k_f}{2\pi k_i} \sum_{\nu\nu'} a_\nu a_{\nu'} \int e^{-iEt} \exp[i\vec{\kappa}(\vec{b}_\nu - \vec{b}_{\nu'})] \prod_\lambda \langle \chi^{(\lambda)}_{\nu\nu'} \rangle_T \, dt$$

with $$\langle \chi^{(\lambda)}_{\nu\nu'} \rangle_T = \exp\left\{ -\left[(\vec{\kappa}\vec{c}^{\,\lambda}_\nu)^2 + (\vec{\kappa}\vec{c}^{\,\lambda}_{\nu'})^2\right] \frac{\coth \frac{\omega_\lambda}{2T}}{4\omega_\lambda} \right\} +$$

$$+ \sum_{n_\lambda=-\infty}^{\infty} e^{i n_\lambda \omega_\lambda t} \cdot e^{-\frac{n_\lambda \omega_\lambda}{2T}} \cdot I_{n_\lambda}\left(\frac{(\vec{\kappa}\vec{c}^{\,\lambda}_\nu)(\vec{\kappa}\vec{c}^{\,\lambda}_{\nu'})}{2\omega_\lambda \sinh \frac{\omega_\lambda}{2T}} \right)$$

A system of units is employed in which $\hbar$ has unit magnitude and T is measured in units of energy. $\vec{k}_i$, $\vec{k}_f$, the initial and final neutron momentum. $E = E_i - E_f$, the energy transfered to the neutron upon scattering.

For small arguments, the modified Bessel functions can be approximated by

$$(2)\quad I_n(x) \cong \left(\tfrac{1}{2}x\right)^{|n|} (|n|!)^{-1}$$

We specialize now and consider only the incoherent partial differential cross section for elastic scattering and the one quanta processes :

$$(3)\quad \frac{d^2\sigma}{d\Omega\, dE} = \frac{k_f}{2\pi k_i} \sum_\nu a_\nu^2 \int e^{-iEt} \prod_\lambda \exp\left\{ -2(\vec{\kappa}\vec{c}^{\,\lambda}_\nu)^2 \frac{\coth \frac{\omega_\lambda}{2T}}{4\omega_\lambda} \right\} +$$

$$+ \left[I_0\left(\frac{(\vec{\kappa}\vec{c}^{\,\lambda}_\nu)^2}{2\omega_\lambda \sinh \frac{\omega_\lambda}{2T}} \right) + e^{i\omega_\lambda t} \cdot e^{-\frac{\omega_\lambda}{2T}} \cdot I_1\left(\frac{(\vec{\kappa}\vec{c}^{\,\lambda}_\nu)^2}{2\omega_\lambda \sinh \frac{\omega_\lambda}{2T}} \right) \right] dt$$

The cross section for <u>elastic scattering</u> is therefore given by :

$$(4)\quad \left(\frac{d\sigma}{d\Omega}\right)_{el} = \sum_\nu a_\nu^2 e^{-2W_\nu} \cdot \prod_\lambda I_0\left(\frac{\varphi W_\nu^\lambda}{\omega_\lambda \coth \frac{\omega_\lambda}{2T}}\right)$$

Here W_ν^λ is the contribution of each mode to the Debye Waller exponent. For a regular lattice with $3N$ normal modes, W is of the $O(\frac{1}{N})$ therefore, if one considers only one phonon process $I_o(o) = i$ and the elastic scattering depends only on the Debye Waller factor $\exp(-2W)$. However, if there are "Local" modes, that give a considerable contribution to the Debye Waller exponent, then the elastic scattering is given by equation (4).

For the <u>incoherent inelastic cross section</u> of any given excitation process one can write by approximating $I_o \simeq 1$:

$$(5)\quad \frac{d^2\sigma^{inc}}{d\Omega dE} = \frac{k_f}{k_i}\sum_\nu a_\nu^2 \left[\prod_\lambda \exp\left\{-\varphi(\vec{H}\vec{e}_\nu^\lambda)^2 \frac{\coth\frac{\omega_\lambda}{2T}}{4\omega_\lambda}\right\}\right] \times e^{-\frac{\omega_\lambda}{2T}} \cdot I_1\left(\frac{(\vec{H}\vec{e}_\nu^\lambda)^2}{\varphi\omega_\lambda \sinh\frac{\omega_\lambda}{2T}}\right) \times \delta(\omega_\lambda -$$

For all possible oscillations in a given system, one finds :

$$(6)\quad \frac{d^2\sigma^{inc.}}{d\Omega dE} = \frac{k_f}{k_i}\sum_\nu a_\nu^2 e^{-2W_\nu} \cdot \sum_{\omega_\lambda} e^{-\frac{\omega_\lambda}{2T}} \cdot I_1\left(\frac{(\vec{H}\vec{e}_\nu^\lambda)^2}{\varphi\omega_\lambda \sinh\frac{\omega_\lambda}{2T}}\right) \delta(\omega_\lambda - E)$$

with $$W_\nu = \sum_\lambda (\vec{H}\vec{e}_\nu^\lambda)^2 \frac{\coth\frac{\omega_\lambda}{2T}}{4\omega_\lambda}$$

the Debye Waller exponent.

Using the quasi continuous benaviour of thé frequency distribution, we can replace $\sum_{\omega_\lambda} \rightarrow \int g(\omega) d\omega$ and obtain by approximating $I_\lambda(x) \approx \frac{1}{2} X$:

$$(7)\quad \frac{d^2\sigma_{inc.}}{d\Omega\, dE} = \frac{k_f}{k_i} \sum_\nu a_\nu^2 e^{-2W_\nu} \cdot \sum_{\omega_\lambda} e^{-\frac{\omega_\lambda}{2T}} \cdot \frac{1}{2} \cdot \frac{(\vec{H}\vec{e}_\nu^\lambda)^2}{\omega_\lambda \sinh \frac{\omega_\lambda}{2T}} \cdot \delta(\omega_\lambda - E)$$

$$= \frac{k_f}{k_i} \sum_\nu a_\nu^2 e^{-2W_\nu} \frac{(\vec{H}\vec{e}_\nu^\lambda)^2}{4E} \cdot \frac{e^{-\frac{E}{2T}}}{\sinh \frac{E}{2T}} \cdot g(E)$$

$$= \frac{1}{2} \frac{k_f}{k_i} \cdot \frac{g(E)}{E} \cdot \frac{1}{e^{\frac{E}{T}} - 1} + \sum_\nu a_\nu^2 e^{-2W_\nu} |\vec{H}\vec{e}_\nu(E)|^2$$

Assuming an isotropic Debye Waller exponent, one obtains the usual cross section formula with $a_{incoh}^2 = \frac{\sigma_{inc}}{4\pi}$

$$8)\quad \frac{d^2\sigma}{d\Omega\, dE} = \frac{1}{8\pi} \cdot \frac{k_f}{k_i} \cdot \frac{\vec{H}^2}{E} \cdot \frac{1}{e^{\frac{E}{T}} - 1} \cdot g(E) + \sum_\nu \sigma_\nu^{inc} e^{-2W_\nu} |e_\nu(E)|^2$$

$$= F(E) \cdot g(E) + \sum_\nu \sigma_\nu^{inc} \cdot e^{-2W_\nu} |e_\nu(E)|^2$$

$$= F(E) \cdot G(E)$$

with

$$F(E) = \frac{1}{8\pi} \cdot \frac{k_f}{k_i} \cdot \frac{\vec{H}^2}{E} \cdot \frac{1}{e^{\frac{E}{T}} - 1}$$

$$G(E) = g(E) + \sum_\nu \sigma_\nu^{inc}\, e^{-2W_\nu} |e_\nu(E)|^2$$

G(E) : the generalized frequency distribution function.

I.1. The amplitude dependence of the impurity atom in the "Band" frequency range

The two component systems VH_n is quite suited to measure by inelastic neutron scattering, the energy dependence of the amplitude of the impurity. Both elements, V and H, scatter neutrons almost entirely incoherently and therefore all nuclei make additive contributions to the scattered intensity. Hence it is possible to determine the energy dependent intensity ratio,

$$(9) \qquad \frac{\mathcal{J}_{V+I}(E) - \mathcal{J}_V(E)}{\mathcal{J}_V(E)} = \frac{\mathcal{J}_H(E)}{\mathcal{J}_V(E)} \sim |\vec{C}_H(E)|^2$$

Using (8), we can evaluate the magnitude for $C_H(E)^2$ for the band modes by :

$$\mathcal{J}(E) = \mathcal{F}(E) \cdot \mathcal{g}(E) * \sum_\nu \sigma_\nu^{inc} e^{-2W_\nu} |\vec{C}_\nu(E)|^2$$

$$(10) \qquad \mathcal{J}_V(E) = \mathcal{F}(E) \cdot \mathcal{g}(E) \cdot \sigma_V^{inc} \cdot e^{-2W_V} \cdot N_V |C_V(E)|^2$$

$$(11) \qquad \mathcal{J}_{V+I}(E) = \mathcal{F}(E) \cdot \mathcal{g}(E) \cdot \left[\sigma_V e^{-2W_V} \cdot N_V |C_V(E)|^2 + \sigma_{+,I} \cdot e^{-2W_H} N_H \cdot |C_H(E)| \right.$$

where $N = N_V + N_H$, N_V, N_H are the number of atoms in the sample. For Vanadium we have the normalisation condition :

$$(12) \qquad \sum_V |C_V(E)|^2 = \frac{1}{M_V} \qquad (M_V = \text{Mass of Vanadium atom})$$

For Vanadium Hydride, we have a different normalisation condition :

$$(13) \qquad M_V N_V |C_V(E)|^2 + m_H N_H |C_H(E)|^2 = 1$$

Assuming isotropic distributions of the H-amplitudes in the VH_n-lattice, we obtain from equation (10), (11), (12) and (13) the energy dependent amplitude ratio :

$$(14)\quad \left|\frac{C_H(E)}{C_V(E)}\right|^2 = R(E) + \frac{N_V \sigma_V}{N_H \cdot \sigma_H} + e^{\varphi\left(W_H(E_0) - W_V(E_0)\right)} \frac{E + \varphi E_0}{2E_0}$$

with

$$R(E) = \frac{\mathcal{F}_{VH}(E) - \mathcal{F}_V(E)}{\mathcal{F}_V(E)}$$

for scattering at 90° angle and E_o the energy of the impinging neutrons.

In Fig. [11], R(E) and $\frac{C_H(E)^2}{C_V(E)}$ are given.

This result can be compared with the calculations of Dawber and Elliott [7] by using an effective mass ratio :

$$\mathcal{E}_{eff} = 1 - \frac{M_H}{M_V} \cdot \frac{\alpha_V}{\alpha_H} = 0.84.$$

The effective mass ratio is introduced because of the experimental evidence, that $\omega_H^{Local} / \omega_V^{max} \approx 2.5$ and not 7 as one would expect from $\sqrt{\frac{M_V}{M_H}}$. Hence we can assume that the force constant of Hydrogen is approximately 1/8 = $\frac{\alpha_H}{\alpha_V}$ of the force constant of Vanadium. For a frequency ratio of $\omega_H^{Band} / \omega_V^{max} \approx 0.6$ and $\mathcal{E}_{eff} = 0.84$, Dawber and Elliott [7] find for $\left|\frac{C_H}{C_V}\right|^2 \approx 0.6$, a value about 2.5 times smaller than the measured one; $\left|\frac{C_H}{C_V}\right|^2_{measured}$ (E = 25 meV) = 1.48. This large deviation cannot be understood easily. With the present day data, we cannot exclude completely the existence of multiphonon processes in the band mode region, that could be responsible for the experimental value large than 1. However the intensity contributions due to multiphonon processes should occur primarily in the energy region between 50 - 100 meV if the local mode with the lowest energy occurs at 100 meV.

Since the amplitudes of the H-atoms for the band mode region should be of the same order as of the Vanadium atoms, the multiphonon processes, due to combinations of band modes, should be negligeable or similar as in the case of Vanadium. A detailed analysis will be given later in the paper.

It is quite possible that the large value for $\left|\frac{C_H}{C_V}\right|^2 = 1.48$ is coming from the approximation $\prod_\lambda I_o = 1$.

Since we do have a very strong localization of the hydrogen, one should include the factor $\prod_\lambda I_o(X_\lambda)$ that was made unity in the derivation of equation 8, 11 and 14. Therefore formula 14 should be written :

$$(15)\quad \left|\frac{C_H(E)}{C_V(E)}\right|^2 = R(E) + \frac{N_V \sigma_V}{N_H \sigma_H} + \frac{e^{\varphi(N_H(E_0)-N_V(E_0))\frac{E+\varphi E_0}{\varphi E_0}}}{\prod_\lambda I_o\left(\frac{\varphi W_\lambda}{\cosh \frac{\omega_\lambda}{2T}}\right)}$$

In our measurement we do not have 3 local modes but because of the relative large concentration we might have a large number of local modes or some modes with particular large amplitudes that could make the product $\prod_\lambda I_o > 1$ and therefore account for the deviation.

To improve the present experimental results, experiments will be carried out at smaller scattering angle and low temperature in order to test the present, preliminary, results on $\left|\frac{C_H}{C_V}\right|^2$ and also to extend the useful range itself.

I.2. The "quasi elastic" Scattering

As already mentioned, a finite life time of the "local" modes could cause a quasi elastic peak, if the contributions of the "local" modes to the elastic scattering is predominant.

This could be the case if no "band" modes are observed and therefore all the elastic scattering due to the "local" modes. However, in our case, the band modes contribute most to the inelastically scattered neutron intensity; hence one has to examine if the contributions of the "local" modes to the elastic scattering are sufficient to follow such a hypothesis.
Using (3) we try to estimate $\mathcal{J}_{H_{elastic}}^{Local} / \mathcal{J}_{H_{elastic}}^{Band}$.

Evaluating (3) we obtain for elastic and inelastic scattering

$$(16a)\quad \left(\frac{d\sigma}{d\Omega}\right)_{el} = \mathcal{J}_{H\,elastic} = N_H b_H^2 e^{-2W_H(E_0)} \prod_\lambda I_0(x_\lambda)$$

$$(16b)\quad \frac{d^2\sigma}{d\Omega\, dE} = \mathcal{J}_{H\,inelastic} = N_H b_H^2 \sqrt{\frac{E+E_0}{E_0}}\, e^{-2W_H(E_0)\left(\frac{E}{2E_0}+1\right)} e^{-\frac{E}{2T}} I_1(x_\lambda)$$

Using (16) we write :

$$(17)\quad \frac{\mathcal{J}_{H_{inelastic}}^{Band}}{\mathcal{J}_{H_{elastic}}^{Band}} = \sqrt{\frac{E_B+E_0}{E_0}}\, e^{-W_H(E_0)\frac{E_B}{E_0}} e^{-\frac{E_B}{2T}} I_1\left(\frac{2W_B}{\omega_\lambda \frac{\omega_B}{2T}}\right)$$

W_B is the contribution of a band mode to the Debye Waller exponent.
Since $W_B \approx O(\frac{1}{N})$, we have practially $I_0(X_B) = 1$.

$$(18)\quad \frac{\mathcal{J}_{H_{(inelastic)}}^{Local}}{\mathcal{J}_{H_{(elastic)}}^{Local}} = \sqrt{\frac{E_L+E_0}{E_0}}\, e^{-W_H(E_0)\frac{E_L}{E_0}} e^{-\frac{E_L}{2T}} + \frac{I_1\left(\frac{2W_L}{\omega_\lambda/2T}\right)}{I_0\left(\frac{2W_L}{\omega_\lambda/2T}\right)}$$

For local modes, the contribution to the Debye Waller exponent can be considerable and $I_0(X_L) \geq 1$.

With (17) and (18) we get :

$$(19)\quad \frac{f^{Local}_{H_{(elastic)}}}{f^{Band}_{H_{(elastic)}}} = \frac{f^{Local}_{H_{(inelastic)}}}{f^{Band}_{H_{(inelastic)}}} \cdot \sqrt{\frac{E_B + E_o}{E_L + E_o}} \cdot \frac{I_1(x_B) \cdot I_o(x_B)}{I_1(x_L)} \cdot e^{W_{H1}(E_o)\left\{\frac{E_L}{E_o} - \frac{E_B}{E_o}\right\}}$$

This intensity ratio can be estimated by using the experimental results in Fig. [3]. We consider only one band frequency ω_B that is obtained by the first moment of the band frequency distribution. The intensity for the two oscillators at ω_L = 110 meV and ω_B = 30 meV is given by the corresponding area under the measured curve. The Debye Waller exponent involved have been estimated by harmonic approximation to $2\,W_L = 0.13$. Using the Rosenstock and Klick relation [17] for an effective mass ratio of $\frac{M_H}{M_V}\frac{\alpha_V}{\alpha_H} = 0.16$ we obtain from W_L for the average contributions of the band modes to the Debye Waller factor $\overline{2\,W_B} = 0.255$.

With these values we get : $I_o(X_L) = 1.03$, $I_1(X_L) = 0.175$, $I_1(X_B)$ 0.108, $f^{Local}_{H_{inel}} / f^{Band}_{H_{inel}} = 0.144$ and $f^{Local}_{H_{(elastic)}} / f^{Band}_{H_{(elastic)}} = 1.2$, a result that supports the hypothesis mode at the beginning.

Therefore it is meaningful to analyse the data under the assumptions of a finite life time of the "local" modes. Hence we consider the differential incoherent scattering cross section in its most general form as given by Van Hove [18].

$$(20)\quad \frac{d^2\sigma}{d\Omega\, dE} = \frac{k_f a^2}{2\pi k_i} \int e^{-iEt} S(\vec{\kappa}, t)\, dt$$

For the hydrogen in the Vanadium lattice $S(\vec{\kappa},t)$ may be thought of as being constituted of possibly only two parts, the "Band" and "Local" modes :

$$S(\vec{\kappa},t) = S_{Band}(\vec{\kappa},t) + S_{Local}(\vec{\kappa},t) \tag{21}$$

From the work of Vineyard [19], we know that the function of $S_B(\vec{\kappa},t)$ reaches its asymptotic form after a small number of mean periods of atomic motions. This has been shown by Vineyard by the calculation of the time dependent square of the width of $S(\vec{\kappa},t)$ for the four cases :
1) gas, 2) ideal liquid, 3) Debye solid, and 4) the harmonic oscillator. The harmonic oscillator $S_L(\vec{\kappa},t)$ has no limit for $t \to \infty$; the contribution of the elastically scattered neutrons will be determined by the average of $S_L(\vec{\kappa},t)$ over a time greater than T, the period of the oscillation : $\overline{S_L(\vec{\kappa},t)} \longrightarrow S_L(\vec{\kappa},\infty)$.

If the local mode has a finite life time τ, we write for (21)

$$S(\vec{\kappa},t) = S_{Band}(\vec{\kappa},\infty) + e^{-\frac{t}{\tau}} S_{Local}(\vec{\kappa},\infty) \tag{22}$$

Physically this means that the local oscillator decays in time either from the "excited" or "ground" state in the collectivized band modes. If one follows consequently, one could expect that the local modes appear and disappear with a certain frequency ν_D, the so called modulation frequency.

The Fourier transform of (22) gives :

$$(23)\quad \frac{d^2\sigma}{d\Omega\, dE} = \frac{k_f}{k_i}\left[\int_{Band} S(\vec{H},\omega)\,\delta(E) + \int_{Local} S(\vec{H},\omega) * \frac{1/\tau}{E^2 + \frac{1}{\tau^2}}\right]$$

The data cannot be fitted with one single τ and S_L. Since the band of local modes is rather wide - and since the proton in the tetrahedral site may oscillate in two frequencies ω_1 and ω_2 - it may be justified that two S_L with two different life times τ_i may be used : τ_1 = 1.5 meV and τ_2 = 3 meV. With $S_{L_1} = S_{L_2}$ = 0.4 S and 0.2 S for purely elastic scattering, one obtaines a qualitative fit to the data shown in Fig. [12]. As already mentioned, experiments are being made with a very high energy resolution to clarify this particular point, that cannot be studied well with the poor energy resolution of the present data.

Within the limits of the theory of lattice dynamics, one cannot expect a physical explanation of the very large diffusion constant of hydrogen in Vanadium. $D \approx 10^{-2}$ cm^2/sec. A proton band model may be a better approach in this respect and probably also as far as the explanation of the very broad "local modes" is concerned. However the apparence of collective "Band" modes is always a direct measure of the degree of localization of the proton in the host lattice matrix.

3.2. The Nb.Hn Data

The measurements on VH_n indicate, that in principle it is possible to deduce from the hydrogen band modes the frequency distribution of the host lattice. This procedure requires at least the knowledge of :

1) The Debye Waller factor for the "Band" and "Local" mode region which can be measured ;

2) The energy dependence of the "Band" mode amplitude of the probe. For coherent scatterer this cannot be determined easily by experiment but it can be taken into account by the Dawber and Elliott connection formula or the Kagan and Josilevskii relation.

We stress this point because it is of interest to know at least approximately the frequency distribution functions for the transition metals. By using a hydrogen probe this could be done at least for the first three elements of each group and Pd, if G(E) will be corrected by expression (15). For Nb and Ta, we can assume, that the energy dependence of the amplitude - similar to Vanadium - is not very strong except at the maximum frequency. Therefore we think that the generalized frequency distribution function as given for Nb in Fig.7 and 8 is quite close to the frequency distribution of Nb if G(E) will be corrected by expression (15). This distribution can be compared with the semi-empirical frequency distribution functions derived by Nakagawa and Woods [20] for Nb; for Tantalum by Woods [21]. Woods used the measured dispersion curves for the high symmetry direction to deduce the frequency distribution with an eight neighbour Born - von Karman force model by calculating the frequencies at 45.526 independent values of $\vec{q}$ in the irreducible 1/48 of the first Brillouin zone.

For Nb two sharp peaks have been found at energies $E_1^{cal} \approx 23.6$ meV $E_2^{cal} \approx 15.8$ meV and a small hump at $E_3^{cal} \approx 4.75$ meV. The small hump at E_3^{cal} is of similar nature as the low energy peak of Vanadium [22].

The neutron distribution for H∠Nb, Fig.7, reveals peaks at $E_1^H = 25.9$ meV, $E_2^H = 18.3$ meV, $E_3^H = 12$ meV. The two peaks E_1^H and E_2^H are slightly higher in energy than E_1^{cal} and E_2^{cal}. This is somewhat surprising since the energy dependence of the H-amplitudes should actually shift the peaks towards lower energies. Since this is not the case, one has to conclude, that the energy dependence of the amplitude is very weak in Nb, except for the max. frequency. The hump $E_3^H = 12$ meV is not seen in the calculated spectra. The energy region E_3^{cal} could not be investigated in the present data due to the overlap from the "quasi elastic" peak. This distribution is similar as in Vanadium hydride.

Since the scattering cross section for Nb is almost entirely coherent, it is of interest to see the deviation of the scattered neutron intensities for Nb, Nb H and (Nb H-Nb). The "band" peaks in the different distributions are clearly shifted. It can be seen in particular for Nb and (Nb H-Nb); a striking effect of the intensity distruction by coherence. These data show at the same time that powder experiments are not suitable to deduce the frequency distribution function. The interference distruction occurs primarily towards the high and low frequency end. The powder measure of coherent scatterers give only information in a certain "window" region.

3.3. The Pd-H_n Data

Apart of the general interest in the formation of "Local" and "Band" modes by the hydrogen impurity, there is a specific interest in the effect of addition of electrons into the electron-bands of the host lattice. In the case of Pd, there are certain indications, that the hydrogen looses its electrons to the electron bands that are supposedly similar instructur as the bands in $Ni(3d^{8}\ 4\ s^{2})$ and that the bare proton is diffusing around in the metal. This view is strongly supported by the measurements of the paramagnetic susceptibility as a function of hydrogen concentration. The susceptibility of the pure metal decreases linearly by the addition of hydrogen until it becomes zero and even slightly negative at concentrations of 65 atom % of hydrogen. This concentration is also about the limiting equilibrium composition that can be achieved at 20°C and 760 mm pressure. Apart of that, the coefficient of the linear term T in the Molar Heat Capacity is very large for Palladium (26-31) x 10^{-4} cal/mole deg^{2} compared to other metals. For these reasons it is of particular interest to measure with neutrons the "Local" and "Band" modes of the proton in Pd as function of H-concentration. In Fig.9 the measure. and corrected data are given. Very striking is the very low local mode energy E_L = 70 meV. The force constant must be quite small as it is also indicated by the very large diffusion coefficient Do = 1.5 x 10^{-2} cm^{2}/sec and the low activation energy of E_D = 6800 cal/g-atom. ($D=Do^{-E_D/RT}$).

The width of the "Local mode" is very strongly concentration dependent : ΔE_L(C=1.5% at) = 40 meV and ΔE_L(C=3% at) = 55 meV; this phenomena is not unexpected as shown by Lengeler and Ludwig [6]. The "Band modes" must have very small amplitudes since they could bearly be seen in the 3% sample. The coupling of the proton to the host lattice must be rather weak as it is also indicated by the low energy of the local mode.

From the neutron diffraction work of Ferguson et al. [23] on β- Pd $H_{0.657}$ we know that the elastic scattering of the hydrogen is increasing with decreasing temperature indicating a stronger binding at lower temperatures. Consequently the band mode amplitude should also increase and therefore it might be possible to measure the band modes by energy loss experiment.

Bergsma and Goedkoop [24] have measured Pd $H_{0.6}$, 60 atom % of hydrogen in Pd, the limiting equilibrium composition at 20°C and 760 mm pressure. The "Local" mode appears at an energy of $E_L(C=60\%) = 57$ meV and a width of $E \sim 47$ meV. The width is about the same as in our 3% sample, but the peak energy is considerable lower. This is a very interesting result, it indicates a peak position dependence on H-concentration, probably it is due to the different phases as our measurements have been made at 3 atom % concentration. However there might be a true peak position dependence on concentration. Such an effect could be qualitatively understood in terms on an increasing correlation of the protons with concentration and consequently an increase of the effective mass or by a weekening of the force constants due to the filling of the 4d-bands in Pd at a concentration of 60%.

3.4. The VD_n-Data

From the neutron measurements in the temperature and concentration range of the phase transition of VH_n, we know that at a concentration of 20 atom % of hydrogen the host lattice is already considerably distorted, this can be seen from the change in shape of the double peak in the host lattice region, Fig. [2]. The measurements on $VD_{0.2}$ reflect the same effect. Therefore by making the difference $VD_{0.2}$ spurious peaks can be produced especially in the host lattice frequency range.

Such an effect is probably responsable for the appearance of the peak in the "Difference-Data", located between the two Vanadium peaks. The local peak of $VD_{0.2}$ (E_L = 88.6 meV) follows approximately the $\sqrt{2}$ relation for the α phase. However there is a considerable change in width of the Local peak $E^L_{VD} \simeq 40$ meV, much smaller than ΔE^L_{VH}. This is not unexpected since the proton or deuterium is sitting in a rather shallow-potential well as it is also suggested by the low activation energy of hydrogen in Nb and Ta.

4. Discussion of the Results for Vanadium Hydride

4.1 Introduction

Hydrogen being an incoherent neutron scatterer the INS+ intensity observed for V-H is the sum of two contributions coming from V and H separately. It is likely that for a small hydrogen concentration, the contribution of vanadium is very similar to the INS intensity due to pure vanadium and is rather well known [14]. The interesting part is therefore the INS intensity scattered by hydrogen, which, in principle, should give information on the motion of hydrogen in metallic lattices, vanadium in our case.

We can think of the hydrogen as sitting in fixed interstitial positions in the vanadium lattice or as moving through a periodic potential due to V ions and electrons, with minima corresponding to these interstitial positions. In the first case, the interpretation of the experimental data is to be sought in the theories of lattices defects as it is developped for example by Montroll, Maradudin and Weiss [23] with corrections taking into account anharmonicity and the possibility of jumps from one position to the next. In the second case, one would start from a calculation of energy bands for the proton supposing that the vanadium ions are held fixed at their equilibrium positions and then try to correct this picture by taking into account the motions of the lattice ions.

+ INS means Inelastic Neutron Scattering, in analogy with NMR, ESR and so on.

Whatever the method of calculation, we believe that the difference experimentally observed between vanadium hydride and the other metal hydrides measured up to now (Zr, Y, Ti) comes from the fact that vanadium has a body centered cubic lattice, instead of a faced centered one like the above mentioned hydrides. This is corroborated by the experiments we have made on niobium and tantalum hydrides, which both are bcc and show a behaviour identical to vanadium hydride, and on the other hand an palladium hydride which behaves more like zirconium hydride.

In both fcc and bcc lattices, a proton or a hydrogen atom (or negative ion) is likely to "stay" in an interstitial position of the octahedral (o) or of the tetrahedral (t) type. These sites are defined in the Table 1. A study of D.N. Beshers [24]
has shown that in bcc it is most probable that small ions like hydrogen ions prefer t-site, contrary to larger ions (C,N) which prefer o-sites. Also neutron diffraction experiments on tantalum deuteride [25] seem to confirm that the t-sites are those occupied by hydrogen. Concerning their interstitial sites the fcc and bcc lattices differ in the following way.

(a) In the bcc lattices o and t-sites are aligned in [100] direction making the chanelling of hydrogen very probable in the three directions [100]. In the fcc lattice no such a situation occurs. The jump of hydrogen from o to t or, o to o, and so on, necessitates the going through the ion cloud, i.e. a very high kinetic energy. A better localization results for fcc lattices.

(b) In the fcc lattice, o and t-sites have the full cubic symmetry, so that a local oscillation of hydrogen is triply degenerate and only one frequency for the localized mode is observed. Instead of that, in the bcc lattices, the o and t-sites have only the tetragonal symmetry, which means that localized oscillations should correspond to two different frequencies, one being doubly degenerate, and the other not degenerate.

These general remarks are elaborated in the following sections.

4.2. A model with localized modes

We assume that the hydrogen is staying permanently in t-site and is linked with its four neighbour vanadium atoms, and that to a first approximation the system is harmonic. It is to be noticed that the harmonic approximation is less valid for vanadium hydride than for pure vanadium, because of the rather large vibration amplitudes of hydrogen for the local modes (as for optic modes). Therefore the harmonic approximation has to be corrected by the anharmonic coupling between the local mode and the band modes.

We know from theory [23] that in the harmonic approximatio the presence of hydrogen, with mass $M_H = 1$, located in the lattice of vanadium atoms mass $M_V = 50.95$ will give rise to normal modes the eigen frequencies $\omega_1, \omega_2, \omega_3$ of which are larger than the maximum frequency ω_m of the band modes, provided that the force constants between hydrogen and vanadium are not too small compared with the force constant in vanadium.

These modes correspond to vibrations of the system in which the amplitudes decreases exponentially from the impurity atom. Because of the large disparity of the masses we shall assume that for these localized modes the exponential decay is so rapid that we can consider the vibration of the vanadium atoms around hydrogen as very small or negligible. This permits to evaluate the mean square displacement $\langle u^2 \rangle$ of the hydrogen by assuming that most of the energy of the local mode is concentrated on the hydrogen atom. If $n(\omega)$ is the Bose occupation number for energy $\hbar\omega$, we have

$$(2.1.) \qquad M_H \omega^2 \langle u^2 \rangle = \left[n(\omega) + \frac{1}{2} \right] \hbar\omega$$

By choosing three orthogonal axes (x, y, z) or (1, 2, 3) parallel to the edges of the cube, and in such a way that z is the 4-fold inversion axis of the t-site, we can write :

$$(2.2.) \quad \langle u_x^2 \rangle = \langle u_y^2 \rangle = \hbar \frac{n(\omega_1) + \frac{1}{2}}{M_H \omega_1} \qquad \langle u_z^2 \rangle = \hbar \frac{n(\omega_3) + \frac{1}{2}}{M_H \omega_3}$$

It is easily seen that if we neglect the motion of vanadium ions and assume central forces between hydrogen and its four nearest neighbouring, then $\omega_1 = \omega_2 = \omega_3 \sqrt{2}$. This equation is still approximately valid if one takes into account the motion of V ions.

For the temperature range used in our experiment, it is a good approximation to neglect $n(\omega_1)$ and $n(\omega_2)$ with respect to 1/2, the frequencies ω_1 and ω_3 being given by

$$(2.3.) \quad \hbar\omega_1 = 105 \text{ meV} \sim 1260 \text{ °K} \qquad \hbar\omega_3 = 75 \text{ meV} \sim 900 \text{°K}$$

The Debye-Waller exponent for hydrogen (DW_e) is defined by

$$2 W_H = \sum_{\alpha\beta} K_\alpha K_\beta \langle u_\alpha(0)\, u_\beta(0) \rangle_T$$

where K_a are the components of the momentum transfer. For tetragonal symmetry, we have :

$$(2.4.) \quad \langle u_\alpha(0)\, u_\beta(0) \rangle_T = \delta_{\alpha,\beta} \langle u_\alpha^2 \rangle ; \quad \alpha,\beta = x,y$$

and thus the contribution of local modes to the DW_e is

$$(2.5.) \quad 2 W_H^{(o)} = \frac{\hbar (K_x^2 + K_y^2)}{2 M_H \omega_1} + \frac{\hbar K_z^2}{2 M_H \omega_3}$$

The exact value of the DW_e depends on the direction of the vector $\vec{K}$ with respect to the z axis of the t-site. An <u>estimate</u> can be obtained by replacing K_x^2, K_y^2, K_z^2 by their average value $\frac{1}{3} K^2$, thus giving

$$(2.6.) \quad 2 W_H^{(o)} = \frac{\hbar K^2}{2 M_H \omega_o} \qquad \frac{1}{\omega_o} = \frac{2}{3\omega_1} + \frac{1}{3\omega_3}$$

$$\hbar \omega_o = 92.6 \text{ meV}$$

If E_o and E are the energy of the incoming and scattered neutron and $\varepsilon = E - E_o$ the energy gain of the neutron we have

$$(2.7.) \quad 2 W_H^{(o)} = \frac{E+E_o}{\hbar \omega_o} = (2W_H)_{\text{elastic}} + \frac{\varepsilon}{\hbar \omega_o}$$

For E_o = 5 meV, $(2W_H)_{\text{elastic}}$ is equal to 0.1 and its value at the highest energy transfer is 1.23.

These values, very large compared with the calculated values for vanadium (0.02 for elastic scattering), mean that the extension cloud of hydrogen, as seen by the neutrons, is very important. It is thus necessary, even in the harmonic approximation to take into account multi-phonon processes, due to combination of the local modes with one another and with the band modes.

As for band modes, we can borrow some conclusions from Elliott and Dawber [7] who have considered the case of an isotopic impurity of mass M' in a cubic lattice with mass M and a Debye spectrum. They have shown that when $\varepsilon = 1 - M'/M$ is positive, the amplitude of the impurity u' is always less than the amplitude u of the host atoms for all in-band modes, the ratio u'/u tending towards unity when the frequency tends to zero. Transposing this into our case, we can assume that for band modes the amplitude of hydrogen u_H is always of the same order as the amplitude of vanadium u_V. The contribution of band modes to the DW_e of hydrogen is therefore of the order of 0.02 for elastic scattering, i.e. negligible compared with the contribution coming from local modes, eq.(2.7.). Besides this, the one-phonon approximation can be considered as valid for the band modes either for vanadium or for hydrogen.

We shall therefore analyze the data on the basis of the Zemach and Glauber (ZG) formalism [13] retaining only the one-phonon terms

---

A.C. Zemach and R.J. Glauber, Phys. Rev. 101, 118 (1965) sect.3

---

for the band modes. We use their notations.

The differential scattering cross section is for coherent case :

$$(2.8.)\quad \sigma(\theta,\varepsilon) = \frac{k}{k_0}\sum_{\nu} a_\nu^2 \frac{1}{2\pi}\int e^{-i\varepsilon t}\prod_{\lambda,L}\langle \chi_{\nu\nu}^{\lambda,L}\rangle dt$$

Where we write λ for band modes and L = 1, 2, 3 for the three local modes with frequencies $\omega_1, \omega_2, \omega_3$. We assume that $\omega_3 < \omega_1 = \omega_2$.

We use the following additional notations :

$$(2.9.)\quad X_\nu^\lambda = \frac{(\kappa . c_\nu^\lambda)^2}{2\omega_\lambda \sinh\left(\frac{\omega_\lambda}{2T}\right)} \qquad W = (\kappa c_\nu^\lambda)^2 (4\omega_\lambda)^{-1}\coth\left(\frac{\omega_\lambda}{2T}\right.$$

$$W_\nu = \sum_\lambda W_\nu^\lambda \qquad n(\omega) = \left[e^{\omega/T} - 1\right]^{-1}$$

$$n^+(W) = n(\omega) + 1 = e^{\omega/T} n(\omega)$$

$$F(\omega) = N\left|c_H(\omega)\right|^2 (2\omega)^{-1} g(\omega) n(\omega)$$

$$F^+(\omega = e^{\omega/T} F(\omega)$$

$$J_0 = I_0(x^1)\, I_0(x^2)\, I_0(x^3) + 2\, I_0(x^3)\, I_1(x^1)\, I_1(x^2$$

$$J_1 = I_0(x^3)\, I_0(x^1)\, I_1(x^2) + I_0(x^3)\, I_0(x^2) I_1(x^1)$$

$$J_3 = I_0(x^1)\, I_0(x^2)\, I_1(x^3)$$

$$J_{13} = I_1(x^3)\, I_0(x^1)\, I_1(x^2) + I_1(x^3)\, I_0(x^2)\, I_1(x^1)$$

We assume that the vectors c_ν^λ are smooth functions of energy and that we can replace $(K.c_\nu^\lambda)^2$ by $K^2\, c_\nu^2(\omega_\lambda)$ due to the symmetry of the crystal and to the fact that we are investigating a powder. $g(\omega)$ is the frequency distribution of the band modes. $I_n(x)$ is a modified Bessel function of order n.

We can write the cross section of hydrogen as a sum over different processes. We are mainly interested by the intensity of neutrons scattered with an energy gain ε, positive and less than ω_1. In this range the contribution to the cross section are proportional to :

a) elastic scattering :

$$J_0 \, \delta(\varepsilon)$$

b) one-phonon scattering :

$$K^2 J_0 F(\omega) \delta(\varepsilon-\omega) + J_1 e^{-\omega_1/2T} \delta(\varepsilon-\omega_1) + J_3 e^{-\omega_3/2T} \delta(\varepsilon-\omega_3)$$

c) two-phonon scattering :

$$K^2 J_1 F(\omega) e^{-\omega_1/2T} \delta(\varepsilon-\omega-\omega_1) + K^2 J_1 F^+(\omega) e^{-\omega_1/2T} \delta(\varepsilon+\omega-\omega_1)$$
$$+ J_{13} \exp\left[-(\omega_1-\omega_3)/2T\right] \delta(\varepsilon-\omega_1+\omega_3)$$

d) three-phonon scattering :

$$K^2 J_{13} \exp\left[-(\omega_1-\omega_3)/2T\right] F^+(\omega) \delta(\varepsilon-\omega_1+\omega_3+\omega)$$

The corresponding cross-sections are obtained by multiplying these quantities by $\frac{k}{k_0} N_H \sigma_H^2 \exp\left[-(2W + 2W^{(o)})\right]$

For Vanadium the only contributions are :

a) the elastic scattering

$$\delta(\varepsilon)$$

b) the one phonon scattering

$$K^2 F_V(\omega) \delta(\varepsilon-\omega)$$

where $F_V(\omega)$ is obtained by replacing $C_H(\omega)$ by $C_V(\omega)$ in $F(\omega)$.

The cross sections are obtained by multiplying these quantities by

$$\frac{k}{k_o} N_V \sigma_V^2 \exp\left[-2 W_V\right]$$

It is easy to obtain an estimate of the multiphonon scattering of hydrogen in the range 22-29 meV. By inspection it is seen that the multiphonon contribution in this range is the three-phonon scattering I_3; the ratio of it to the one-phonon scattering I_1 is given by

$$\frac{I_3}{I_1} = J_{13} \frac{\omega' g(\omega) n(\omega) e^{\omega/2T}}{\omega\, g(\omega') n(\omega') e^{\omega'/2T}}$$

where $\omega' = \varepsilon = \omega_1 - \omega_3 - \omega$

using the value of J_{13} calculated in the Table II, we see that this ratio is of the order of 10^{-3}. We can therefore neglect the multiphonon scattering and compare the data with the one-phonon formula as we have done in preceeding section. We therefore conclude that it is not possible to explain the observed intensity as the basis of a purely harmonic theory with hydrogen on t-sites only.

A first explanation would be that we have a large enhancement of the two and three-phonons processes due to anharmonicity; it is very difficult in the present status of the theory to make any quantitive analyses of the data on this basis.

Another interpretation of these results is that of the two frequencies ω_1, ω_2 of the local modes, one is larger than ω_m and the other is smaller than ω_m giving rise to a resonance of the Brout-Visscher type. This suggestion has been made in another context by Takeno, [25].

4.3. A model with motion of protons in the lattice with a band structure

We observe that the o and t-sites are aligned on straight lines parallel to the [100] directions. If o and t-sites are minima of the potential along this direction, and owing to the geometry of the crystal, the potential hills between minima are not very high, and the o-t lines would behave as open channels for the motion of the proton. We shall assume as a first approximation that the proton is moving in this one dimensional potential, that the vanadium ions are fixed and that the motion of the proton transverse to the channel corresponds to oscillation of very high (200, 300 meV) energy. We shall try to correct for the motion of V ions afterwards.

We, therefore, consider the band structure for the proton moving in a Kronig and Penney [26] potential V(x) defined as follow :

$$V(x) = \begin{cases} 0 & a/2 \leq x \leq 3a/2 \\ -W & -a/2 < x < a/2 \end{cases} \qquad (3.1)$$

V(x) is periodic with the period $a = a_o/4$, the distance between o and t sites. $a_o = 3.028\ A^o$ is the lattice parameter of the cubic cell. We have determined W so that the distance between the lowest energy band (lower band) and the first excited band (upper band) is approximately equal to the observed energy of the high energy peak of VH_x. This gives the value of the depth of the potential.

$$W = 142.5 \text{ meV} \qquad (3.2.)$$

With this value the lower band extends on a range $\Delta E_o = 14$ meV, the bottom of the upper band is separated from the top of the lower band by a gap $E_g = 88.7$ meV and the width of the upper band is $\Delta E_1 = 46.7$ meV. In Fig. [13] we have shown the band structure. We interpret the neutron data by considering :

(a) scattering in which a proton is scattered from a state in the lower band down to another state of the same band. This scattering explains the intensity observed for energy gain in the range 0-14 meV.

(b) scattering in which a proton is scattered down from a state in the upper band to a state in the lower band. This scattering explains the intensity observed for an energy gain in the range 88.7 - 149.4 meV, the peak being centered around 119 meV. A schematic drawing of the intensity scattered is given in Fig. [14].

The exact cross section to be expected from these transitions is somewhat uncertain because it depends on the exact wave function of the proton which is a sensitive function of the exact potential shape. The population factor relevant for the calculation is the Boltzmann factor, since the protons are far from Fermi degeneracy, at room temperature.

We have to add to this picture two features :

First

The vibration of the lattice will drive the proton perpendicularly to the channel direction with its frequency. Thus it is expected to observe an intensity scattered by the proton analogous with the intensity scattered by vanadium in the acoustic modes range, superimposed on the intensity shown in Fig. [14].

Second

The longitudinal vibration of the lattice moving parallel to the channel will induce transitions between states of the Kronig Penney potential. This kind of proton-phonon interaction will give rise to self-energy terms. We can estimate this by evaluating the number of phonons in the phonon cloud around a proton with wave vector $\vec{k}$

$$\langle N \rangle = \frac{M^2 W^2}{(2\pi)^2 \rho c_s \hbar^3 k} \left\{ (q_c - 2k) \ln \left| \frac{q_c - 2k}{q_m + q_c - 2k} \right| \right.$$

(3.2.)

$$\left. + \; (q_c + 2k) \ln \frac{q_m + q_c + 2k}{q_c + 2k} \right\} .$$

With a sound velocity $c_s = 5 \times 10^5$ cm/sec, a density $\rho = 5$, an interaction constant $W = 140$ meV $\approx 0.224\ 10^{-12}$ ergs, we obtain a value $q_c = 2 Mc_s/\hbar = 1.5\ 10^9$ cm^{-1}. We have evaluated $\langle N \rangle$ for the maximum $k = \pi/2a = 4.14\ 10^8$ cm^{-1} and have assumed $q_m = 5.72\ 10^8$ cm^{-1}. The value of $\langle N \rangle$ is then

$$\langle N \rangle = 0.278$$

which means that the phonon-proton interaction is not so large as to invalidate our previous results. At temperature T, the shift to be expected for the maximum value of k is of the order of $\langle N \rangle n(\omega_m) \hbar \omega_m$. At T = 300°K and T = 600°K, we obtain for this thermal broadening of the proton bands :

$T = 300°K$ $\quad\quad \langle N \rangle_{n(\omega_m)} \hbar\omega_m = 2.8$ meV

$T = 600°K$ $\quad\quad \langle N \rangle_{n(\omega_m)} \hbar\omega_m = 9.08$ meV

One sees that this broadening is not negligible compared with the original width of the lower band and that it increases rapidly with temperature.

Position of Metal ions+	o-site	t-site
<u>fcc</u> 000 , $0\ \frac{1}{2}\ \frac{1}{2}$	$\frac{1}{2}\ \frac{1}{2}\ \frac{1}{2}$	$\frac{1}{4}\ \frac{1}{4}\ \frac{1}{4}$
$\frac{1}{2}\ 0\ \frac{1}{2}$, $\frac{1}{2}\ \frac{1}{2}\ 0$	$\frac{1}{2}$ 00 etc.	$\frac{3}{4}\ \frac{1}{4}\ \frac{1}{4}$ etc.
<u>bcc</u> 000 $\frac{1}{2}\ \frac{1}{2}\ \frac{1}{2}$	$\frac{1}{2}\ \frac{1}{2}\ 0$	$\frac{1}{4}\ 0\ \frac{1}{2}$
	0 0 $\frac{1}{2}$ etc.	$\frac{3}{4}\ 0\ \frac{1}{2}$ etc.

<u>Table I</u> : <u>Coordinates of the octahedral (o) and tetrahedral (t) interstitial sites in fcc and bcc lattices</u>

+ cubic cell of edge a.

	elastic	K maximum
J_o	1.000	1.014
J_1	$0.81\ 10^{-2}$	$0.89\ 10^{-1}$
J_3	$1.48\ 10^{-2}$	0.164
J_{13}	$1.44\ 10^{-4}$	$1.74\ 10^{-2}$

Table II : Values of the coefficients J_o, J_1, J_3, J_{13} at T = 300°K for elastic scattering and maximum value of κ

5. Conclusion

Using the hydrogen probe in a crystal, it is possible to deduce from inelastic neutron scattering experiments the generalized frequency distribution $G(\omega)$ of the host lattice. The actual frequency distribution $g(\omega)$ can be obtained by correcting $G(\omega)$ by the energy dependent amplitude of the hydrogen in the host lattice :

$$g(E) = G(E) \left| \frac{1}{C_{hydrogen}} (E) \right|^2 e^{2W_H(E)}$$

For such a procedure the energy dependent amplitude of the impurity atom has to be determined experimentally - as it is possible in vanadium - or theoretically, to be taken into account.

The inelastic scattered neutron distribution can be fairely well understood in terms of the general theory of defect modes. The quasi-elastic scattered neutron distribution can be interpreted by introducing a finit life-time for the local modes.

A proton band theory describes very well the high energy transitions and their corresponding width. The quasi elastic scattered neutrons can be understood as transition in a split ground state level.

—

Acknowledgments
We should like to thank Mr . G. LASALLE for very valuable assistance with the data-handling, Mr. J. ROUSSEAUX for preparing the computor programs and P. DOMINKE for technical assistance.

—

6. Literature

[1] Maradudin A.A., Mazur P., Montroll E.W., and Weiss G.H., Rev. Mod. Phys., Vol.30, 175 (1958)

[2] Takeno S.
Progress of Theoretical Physics, Vol.28, No 1, 33 (1962)

[3] Lifshitz I.M.
Advances in Physics, Vol.13, 483 (1964)

[4] Lifshitz I.M.
Nuovo Cimento, Vol.3, 716 (1956)

[5] Montroll E.W., and Potts R.B.
Phys. Rev. 100, 525 (1955)

[6] Lengeler B. and Ludwig W.
Zeitschrift für Physik, 171, 273 (1963)

[7] Dawber P.G. and Elliott R.J.
Proc. Roy. Soc. A; Vol.273, 222-236 (1963)

[8] Kagan Yu., Josilevskii Ya.
Soviet Phys. JETP, Vol.17, No 4, 925-937 (1963)

[9] Smith S.D. and Angress J.F.
Physics Letters, Vol.6, No 2, 131 (1963)

[10] Stekhanov A.I. and Eliashberg M.B.
Soviet.Phys. Solid State, Vol.5, No 10, 2185 (1964)

[11] Mozer B., Otnes K. and Myers V.W.
Phys. Rev. Letters 8, 278 (1962)

[12] Rubin R., Kley W., and Peretti J.
EUR 522 d

Rubin R., Peretti J., Verdan G. and Kley W.
Physics Letters, Vol.14, No 2, 100 (1965)

[13] Zemach A.C., and Glauber R.J.
Phys. Rev. 101, 118 (1956)

[14] Haas R., Kley W., Krebs K.H. and Rubin R.
Inelastic Scattering of Neutrons in Solids and Liquids,
Vol.II, p.125, IAEA Vienna (1963)

[15] Kazarnovskii M.V. and Stepanov A.V.
Soviet Physics JETP, Vol.20 No 1, 94 (1965)

[16] Mirlin D.N., and Reshina I.I.
Soviet Phys. Solid State, Vol.6, 2454 (1965)

[17] Rosenstock H.B., and Klick C.C.
Phys. Rev. Vol.119, No 4 1198-1203 (1960)

[18] Van Hove L.
Phys. Rev. 95, 249 (1954)

[19] Vineyard G.
Phys. Rev. Vol.110, No 5, 999-1010 (1958)

[20] Nakagawa Y. and Woods A.D.B.
Phys. Rev. Letters, Vol.11, No 6 (1963)

[21] Woods A.D.B.
Phys. Rev. Vol.136, No 3A, A781 (1964)

[22] Ferguson Jr. G.A., Schindler A.I., Tanaka T. and Morita T.
Phys. Rev. Vol.137, No 2A (1965)

[23] Maradudin A.A., Montroll E.W., and Weiss G.H.
Theory of Lattice dynamics in the harmonic approximation
Solid State Physics, Supplement Vol.3

[24] Beshers D.N.
UCRL 7184 University of California 1963

[25] Wallace W.E.
J. Chem. Phys. 35, 2156 (1961)

[26] Takeno S.
Prog. Theor. Phys. 33, 363 (1965)

[27] Kronig de L. R. and Penney W.J.
Proc. Roy. Soc. A 130 499 (1930)

Figure captions

Fig.1 Phase diagram of V-H

Fig.2 Spectra of inelastic scattered neutrons by Vanadium Hydride containing 9 atomic per cent of Hydrogen at 33°C, 70°C, 100°C, 150°C

Fig.3 Time of flight spectra of VH (4 atomic per cent) : —●—●—
V : —○—○—
and (VH-V)=H : --△--△--
at 50°C

Fig.4 Generalized frequency distribution G(E) of
(VH-H)=H : ——
at 50°C

Fig.5 Time of flight spectra of VD (20 atomic per cent): —●—●—
V : —○—○—
and (VD-V)=D : —△—△—
at 50°C (mixed phase range)

Fig.5a Time of flight spectra of VD(20 atomic per cent) : —●—●—
V : —○—○—
and (VD-V)=D : —△—△—
at 150°C (pure α - phase)

Fig.6 Generalized frequency distribution G(E) of
(VD-V)=D : ——
at 50°C (—●—) and
at 150°C(—○—)

Fig.7 Time of flight spectra of NbH(3 atomic per cent) : —●—●—
Nb : —○—○—
and (NbH-Nb)=H : --△--△--
at 33°C

Fig.8 Generalized frequency distribution G(E) of
(NbH-Nb)=H : ——
at 33°C

Fig.9 Time of flight spectra of PdH (1.5 atomic per cent): —●—●—
and Pd —○—○—
at 33°C

Fig.10 Generalized frequency distribution G(E) of
(PdH - Pd = H Pd) : ——
at 33°C

Fig.11 —o—o— : Neutron Intensity Ratio

$$R(E) = \frac{J_{VH}(E) - J_V(E)}{J_V(E)} = \frac{J_H(E)}{J_V(E)}$$

as a function of Energy Transfer at 50°C.

—Δ—Δ— : Ratio of the Hydrogen to Vanadium mean square amplitude as a function to Energy Transfer at 50°C calculated from formula(14).

Fig.12 —o.o— : Time of flight spectrum of (VH-V)=H at 50°C in the elastic range

—Δ—Δ— : The "quasi-elastic" scattered neutron are fitted to a sum of two weighted Lorenzian S1, S2 and anelastic 50 contribution (0,4 S1 + 0,4 S2 + 0,2 S0).

Fig.13 Band structure on V-H model.

Fig.14 Schematic picture of intensity scattered by lower and upper band.

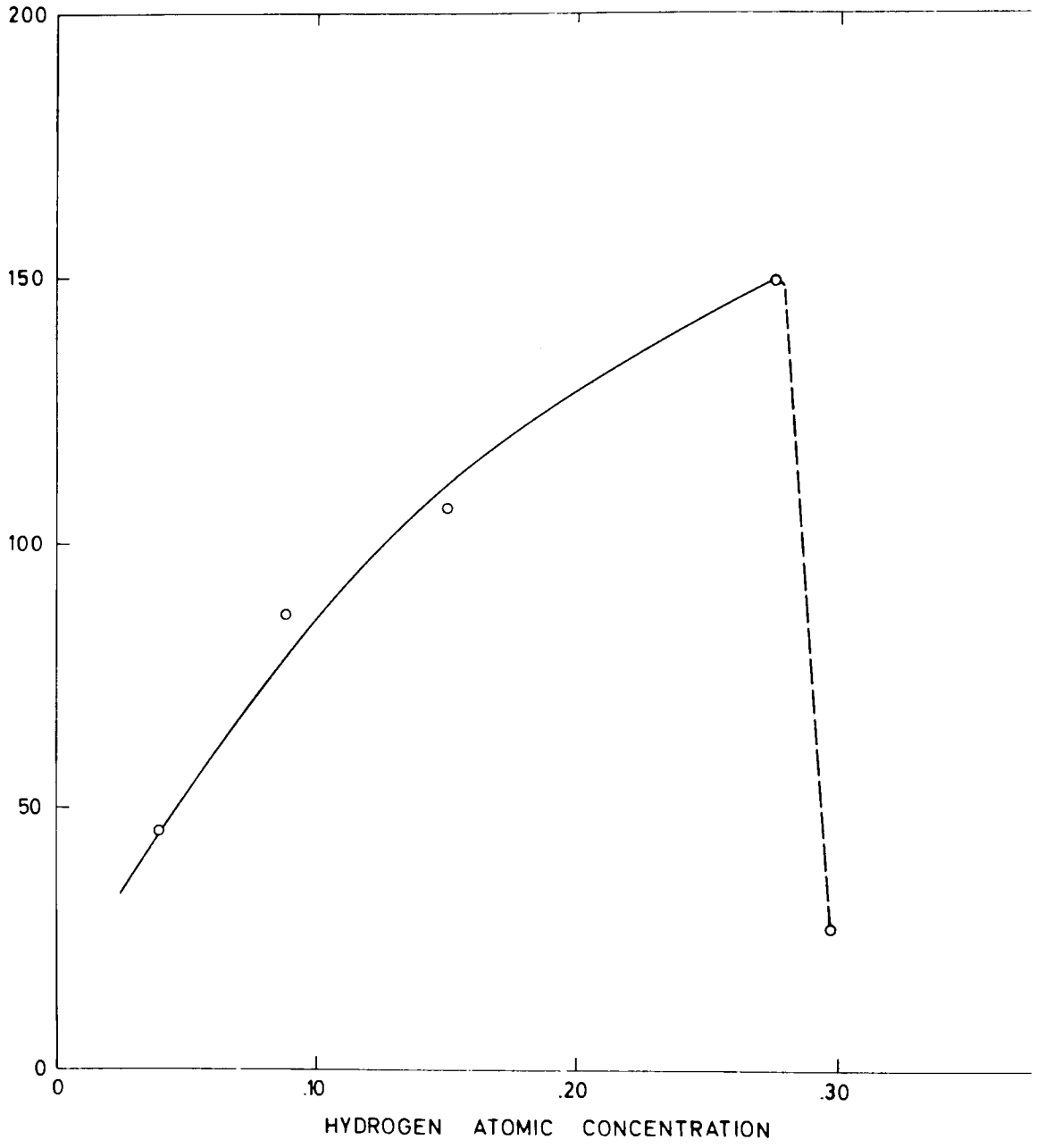

Fig. 1

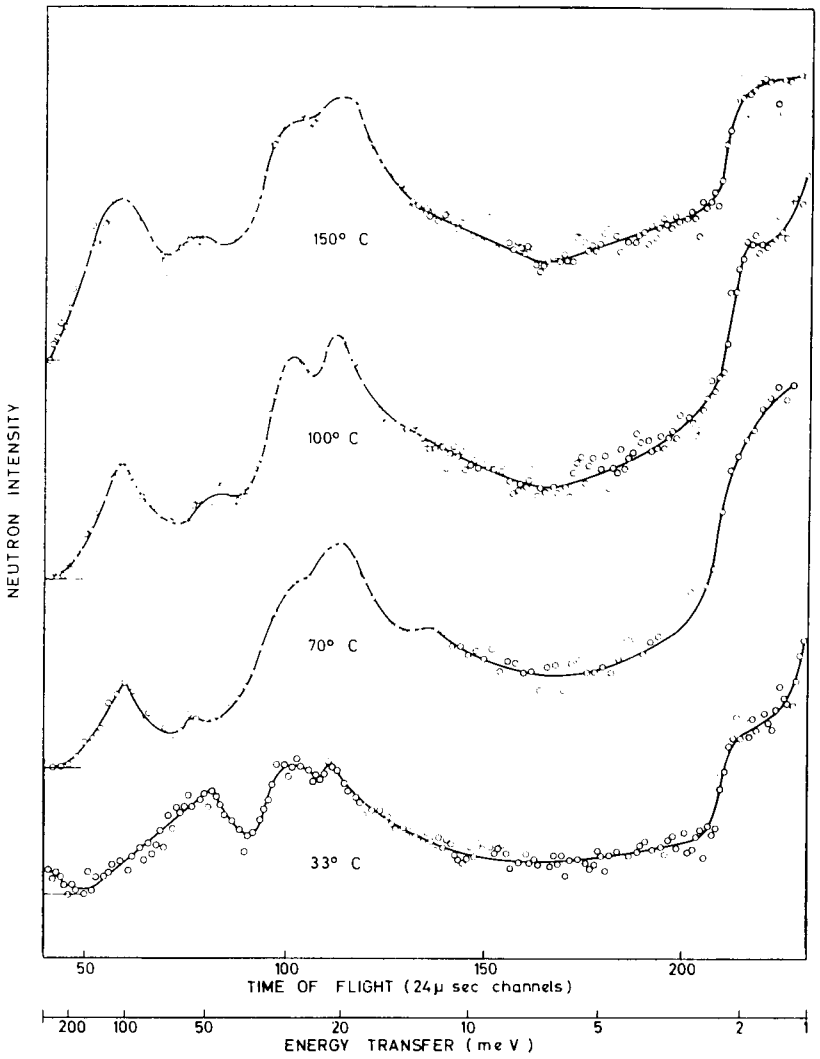
NEUTRON INTENSITY
150° C
100° C
70° C
33° C
50
100
150
200
TIME OF FLIGHT (24μ sec channels)
200
100
50
20
10
5
2
1
ENERGY TRANSFER (meV)

Fig. 2

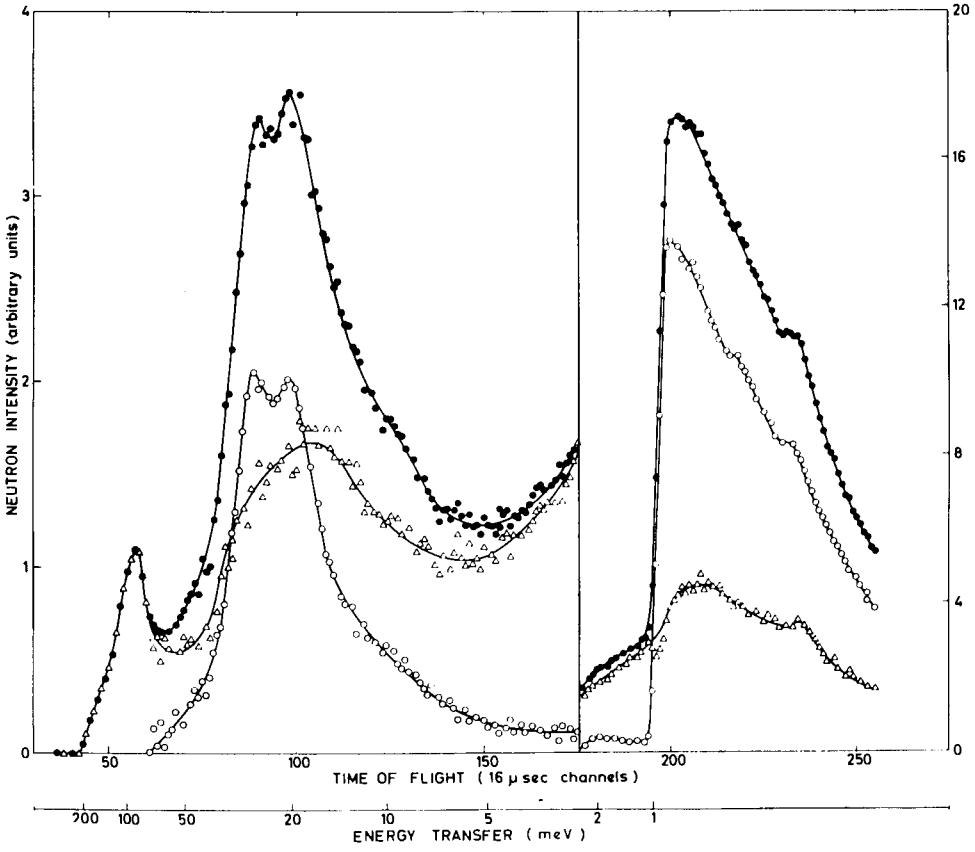
NEUTRON INTENSITY (arbitrary units)
0
1
2
3
4
0
4
8
12
16
20
50
100
150
200
250
TIME OF FLIGHT (16 μ sec channels)
200
100
50
20
10
5
2
1
ENERGY TRANSFER (meV)

Fig. 3

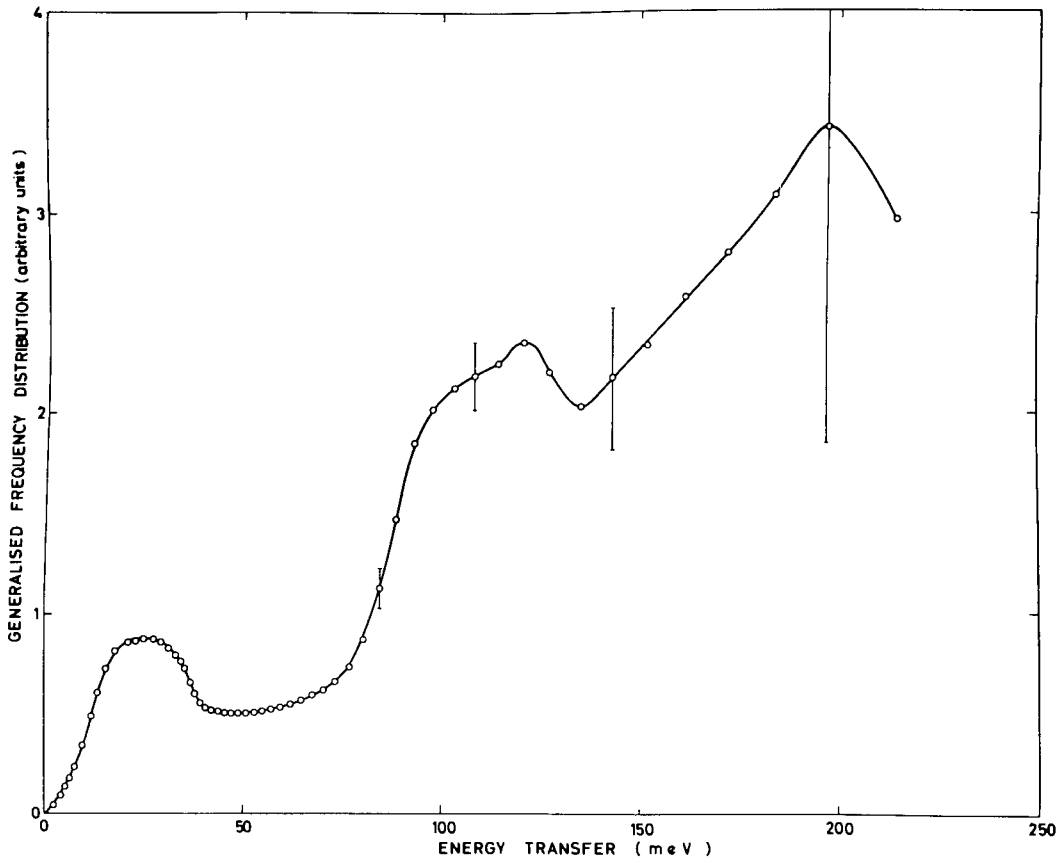
GENERALISED FREQUENCY DISTRIBUTION (arbitrary units)
ENERGY TRANSFER (meV)
0
1
2
3
4
0
50
100
150
200
250

Fig. 4

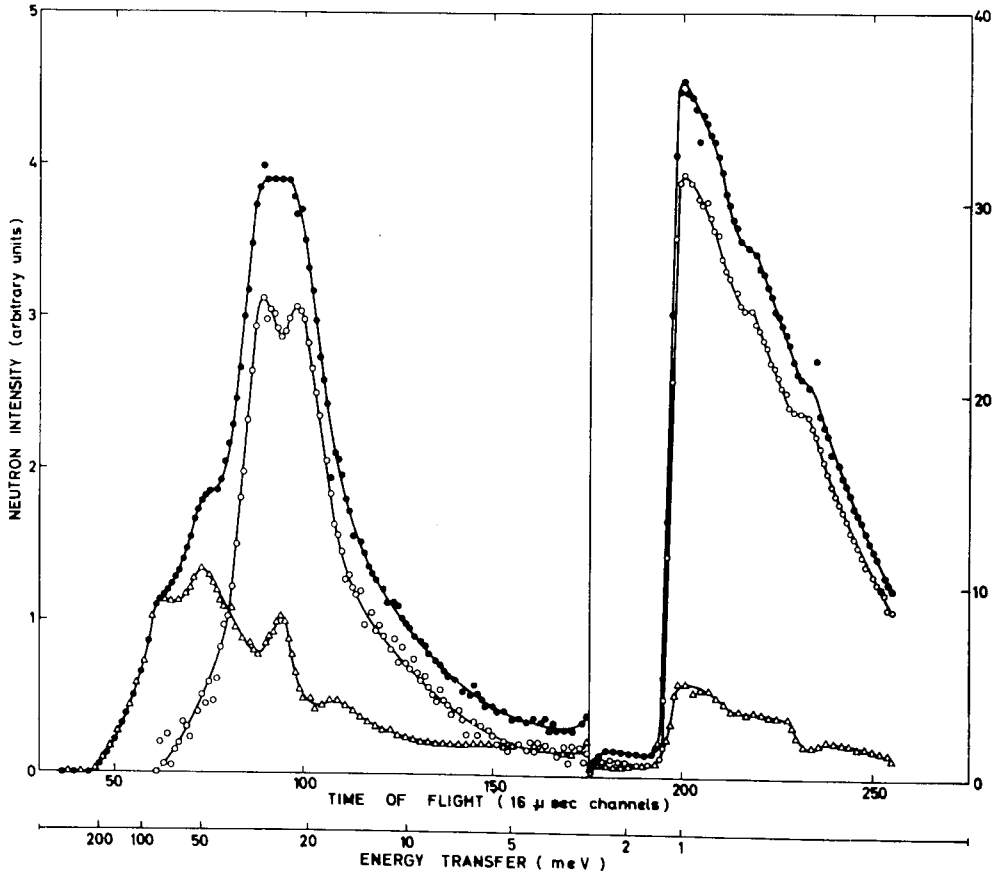
NEUTRON INTENSITY (arbitrary units)
TIME OF FLIGHT (16 μ sec channels)
ENERGY TRANSFER (meV)
0
1
2
3
4
5
0
10
20
30
40
50
100
150
200
250
200
100
50
20
10
5
2
1

Fig. 5

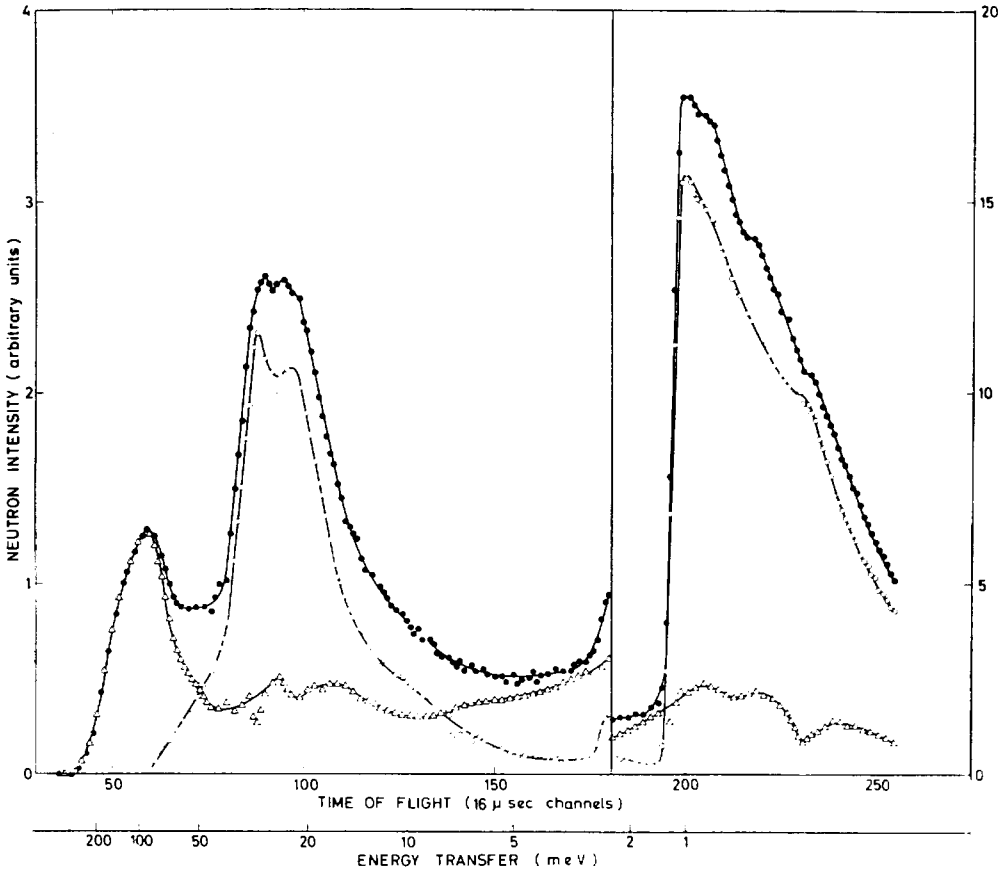
NEUTRON INTENSITY (arbitrary units)
TIME OF FLIGHT (16 μ sec channels)
ENERGY TRANSFER (meV)

Fig. 5 a

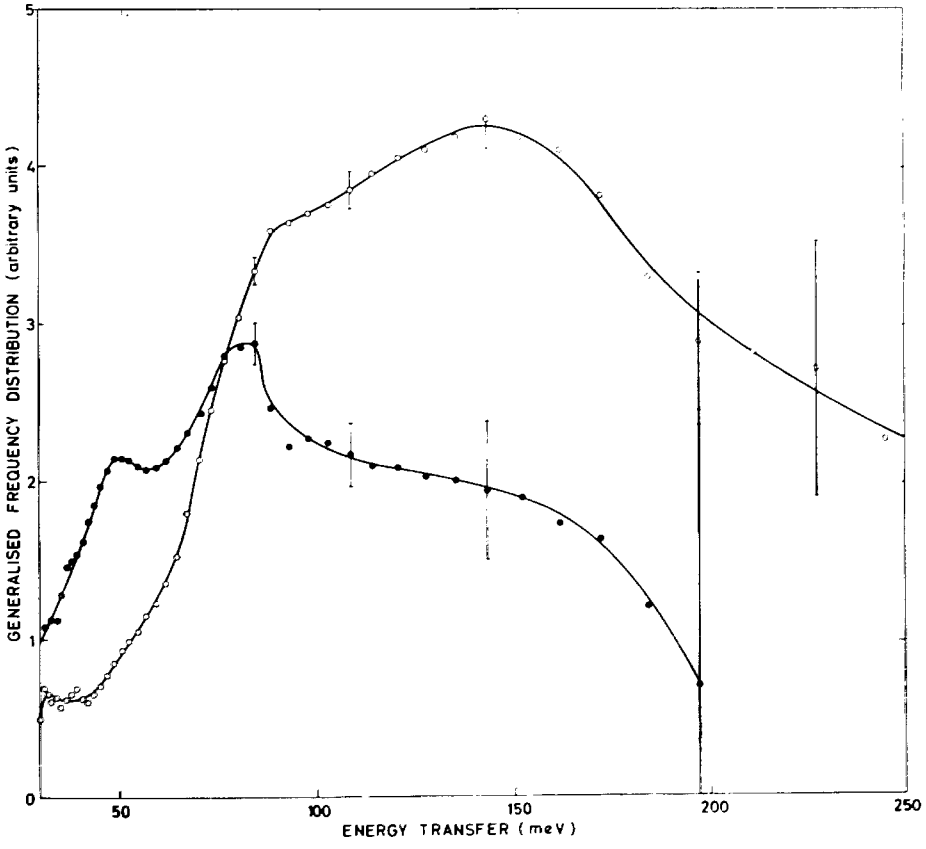
GENERALISED FREQUENCY DISTRIBUTION (arbitrary units)
ENERGY TRANSFER (meV)

Fig. 6

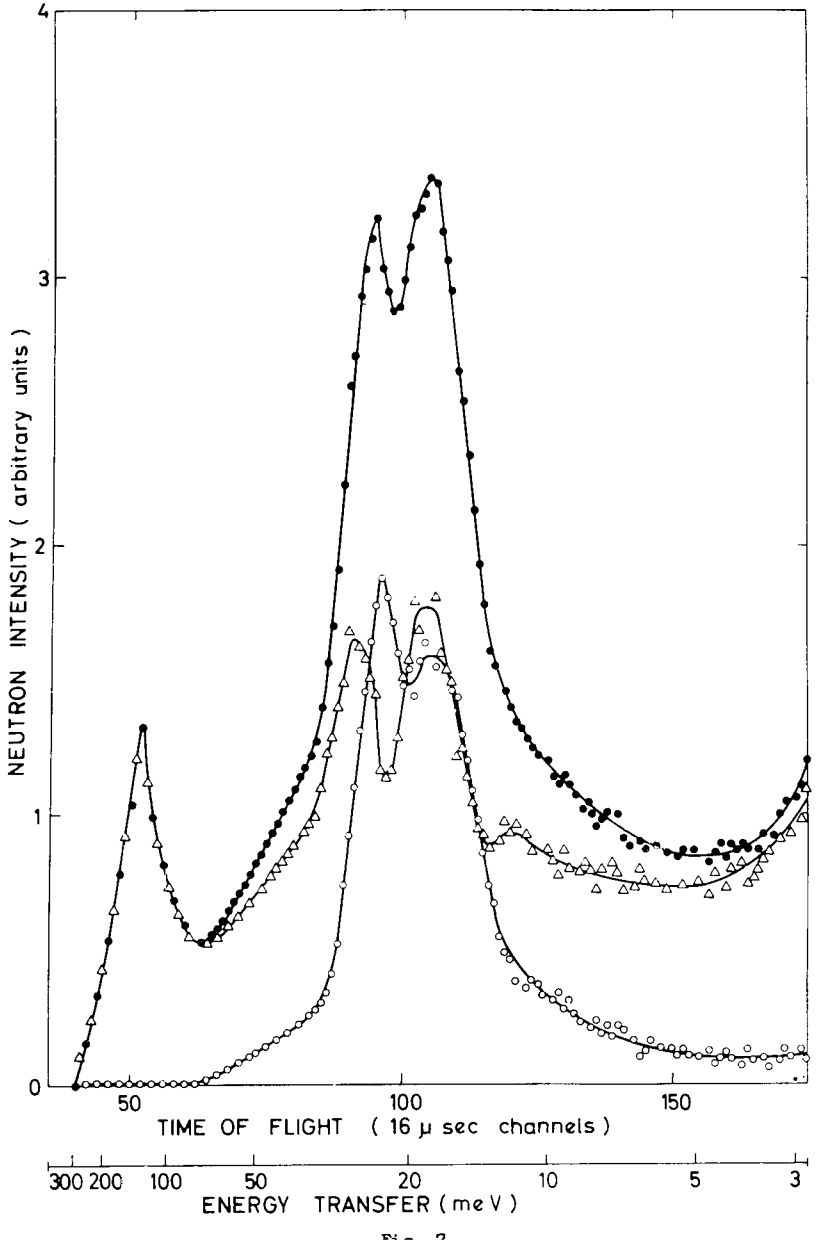
NEUTRON INTENSITY (arbitrary units)
TIME OF FLIGHT (16 μ sec channels)
ENERGY TRANSFER (meV)

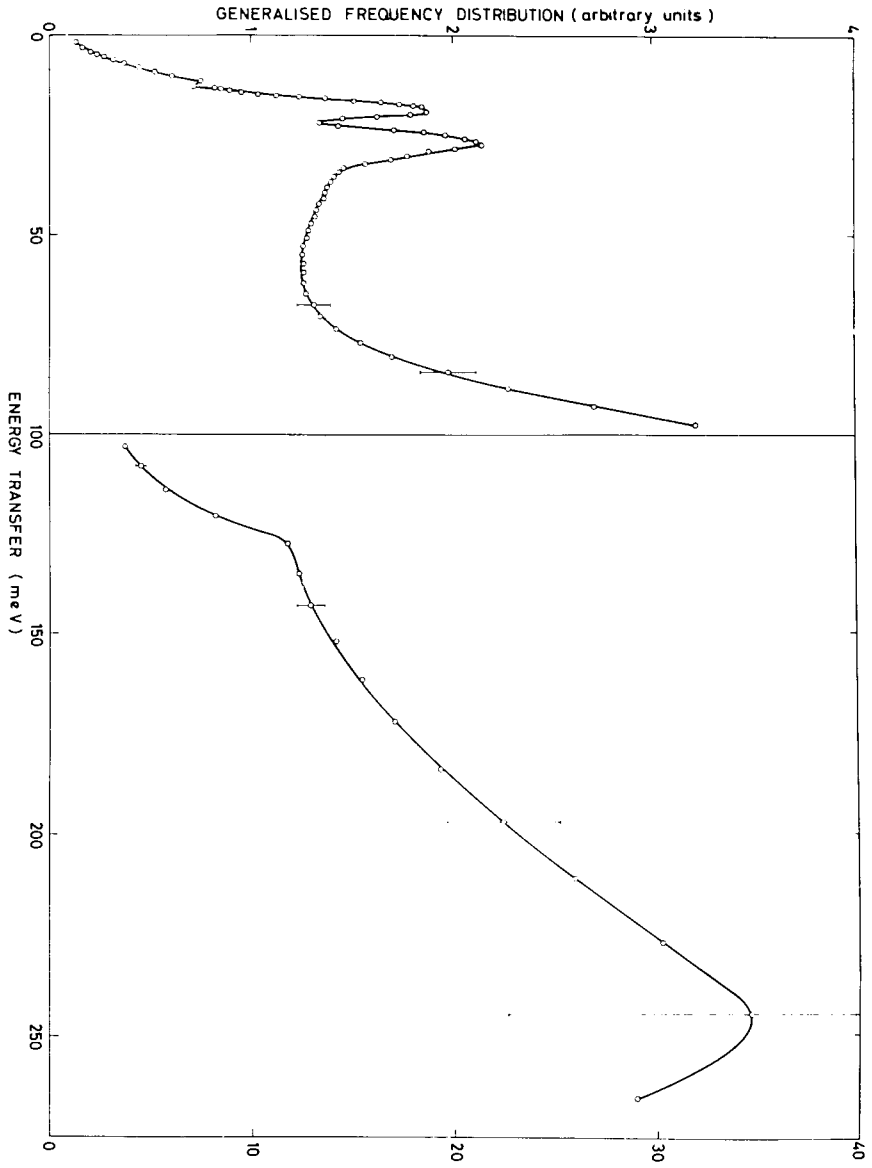
GENERALISED FREQUENCY DISTRIBUTION (arbitrary units)
ENERGY TRANSFER (meV)

Fig. 8

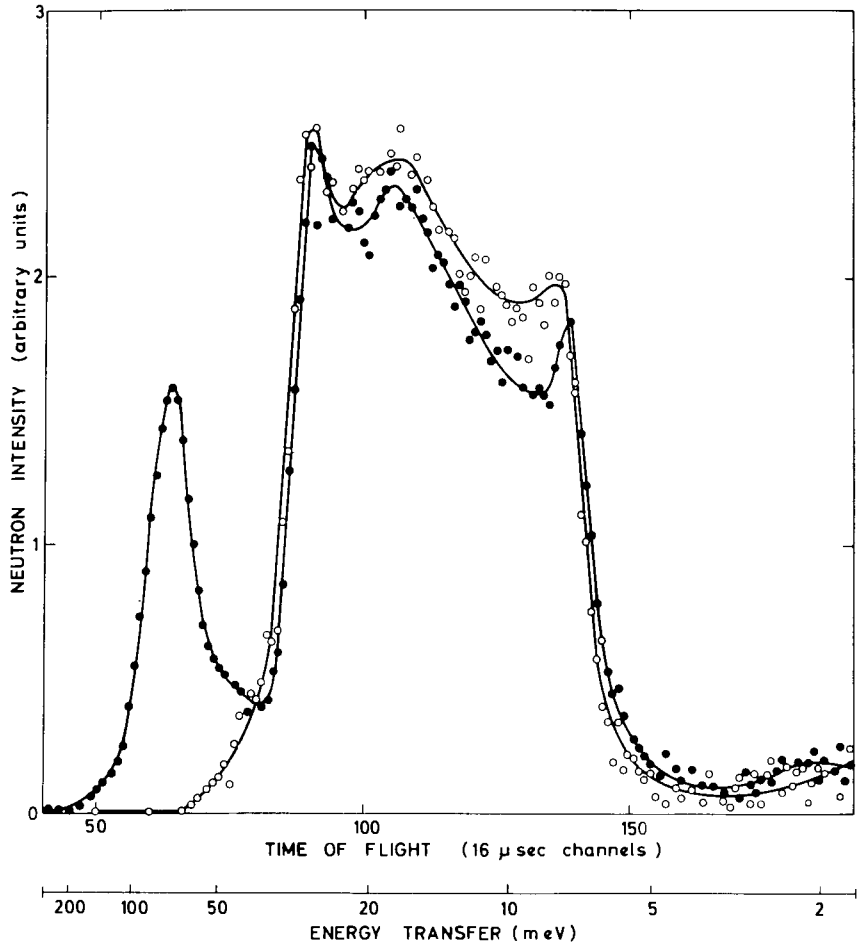
NEUTRON INTENSITY (arbitrary units)
0
1
2
3
50
100
150
TIME OF FLIGHT (16 μ sec channels)
200
100
50
20
10
5
2
ENERGY TRANSFER (meV)

Fig. 9

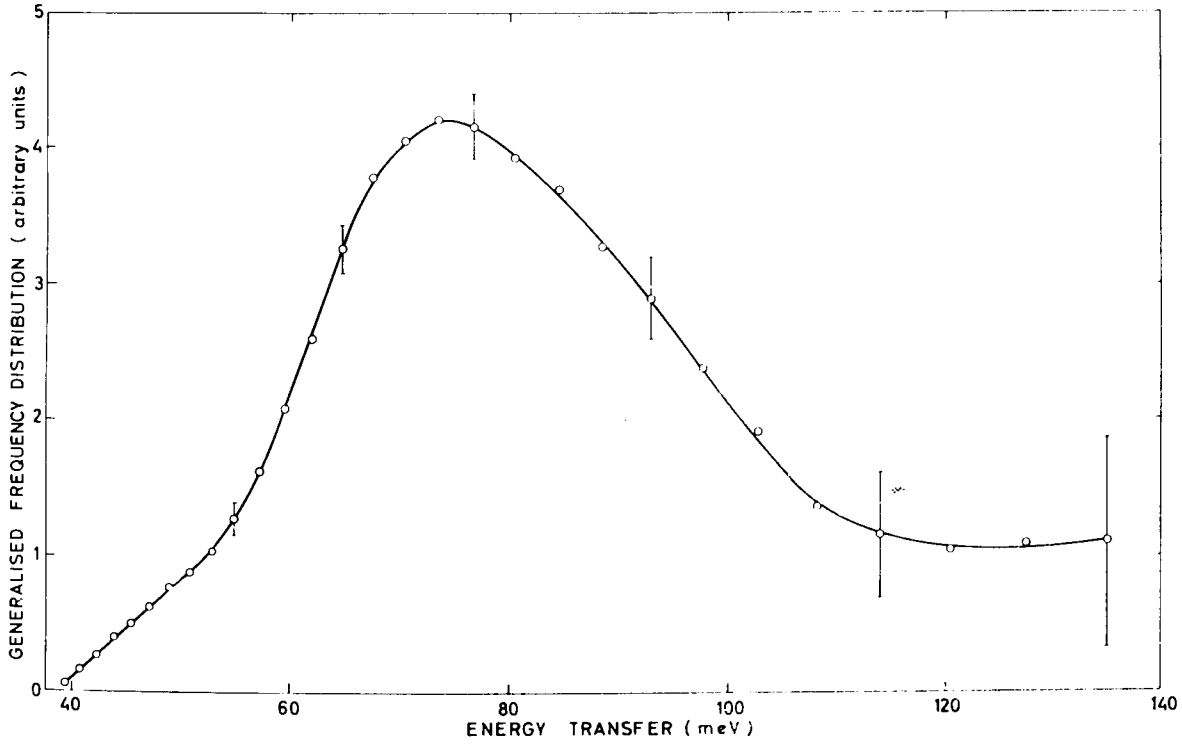
GENERALISED FREQUENCY DISTRIBUTION (arbitrary units)
0
1
2
3
4
5
40
60
80
100
120
140
ENERGY TRANSFER (meV)

Fig. 10

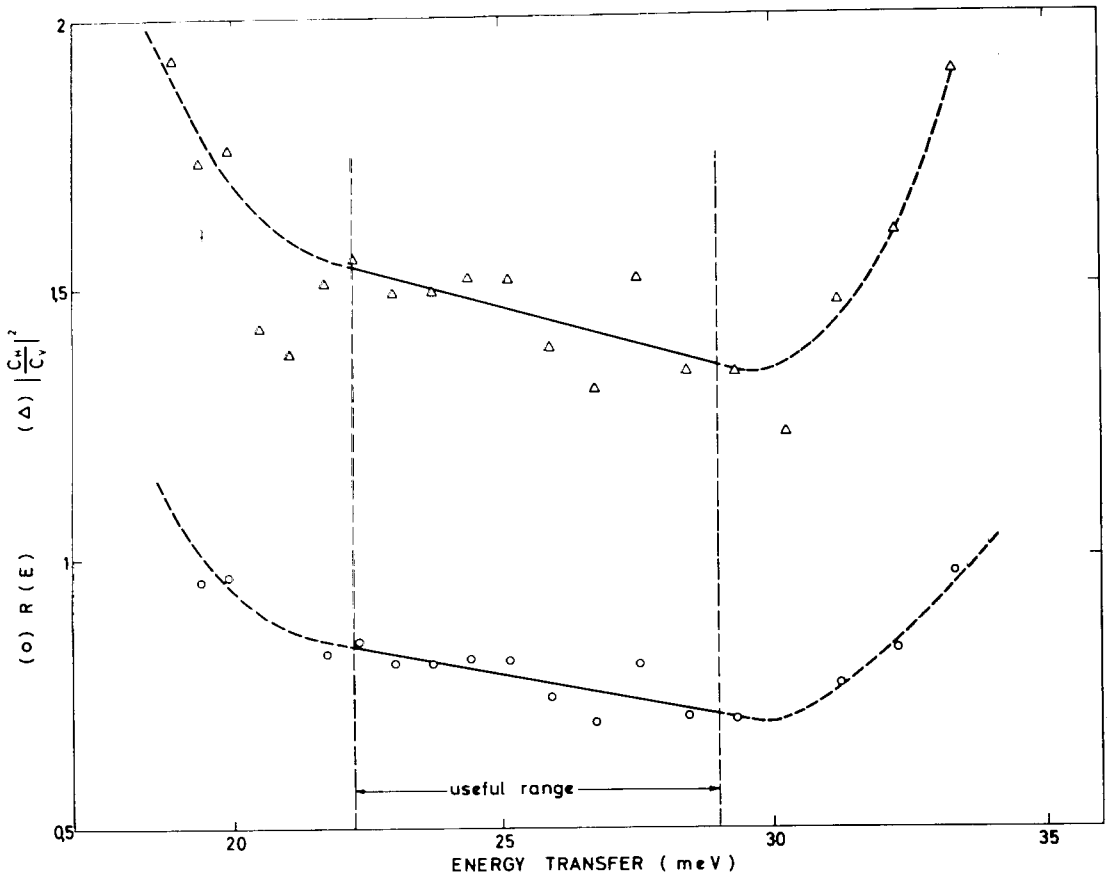
2
1,5
1
0,5
(Δ) $\left|\frac{C_H}{C_V}\right|^2$
(o) R (E)
useful range
20
25
30
35
ENERGY TRANSFER (meV)

Fig. 11

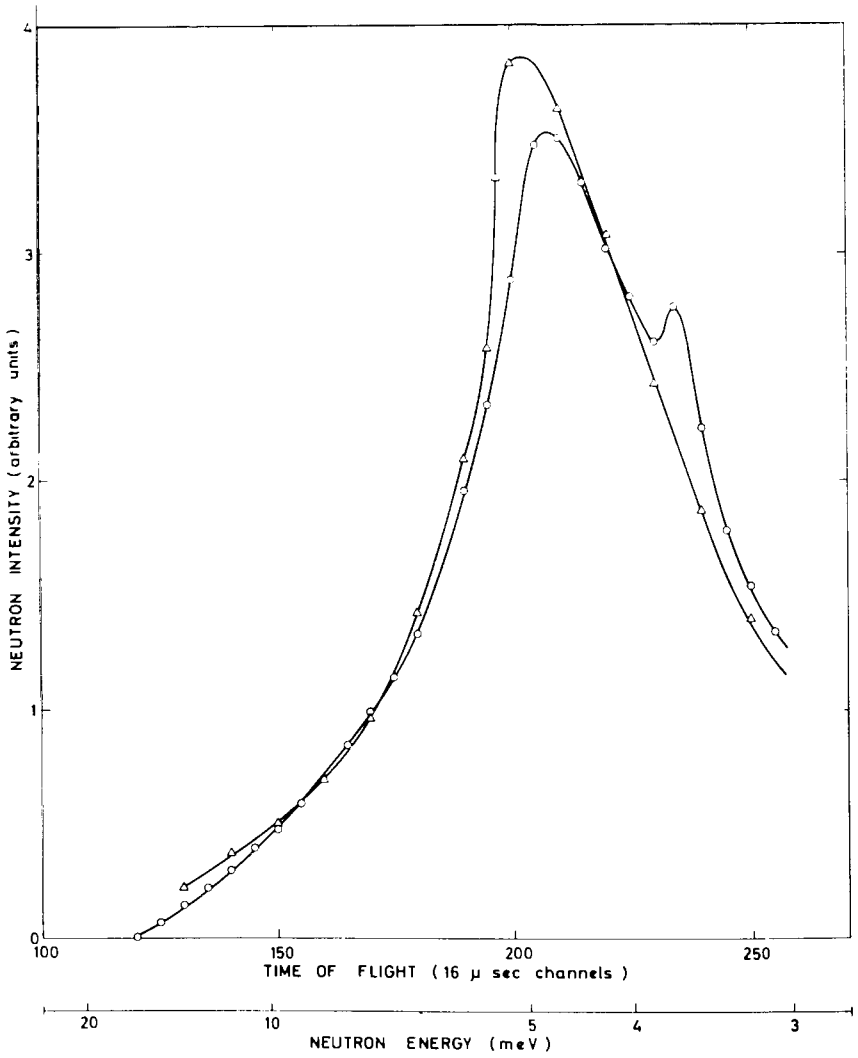
4
3
2
1
0
NEUTRON INTENSITY (arbitrary units)
100
150
200
250
TIME OF FLIGHT (16 μ sec channels)
20
10
5
4
3
NEUTRON ENERGY (meV)

Fig. 12

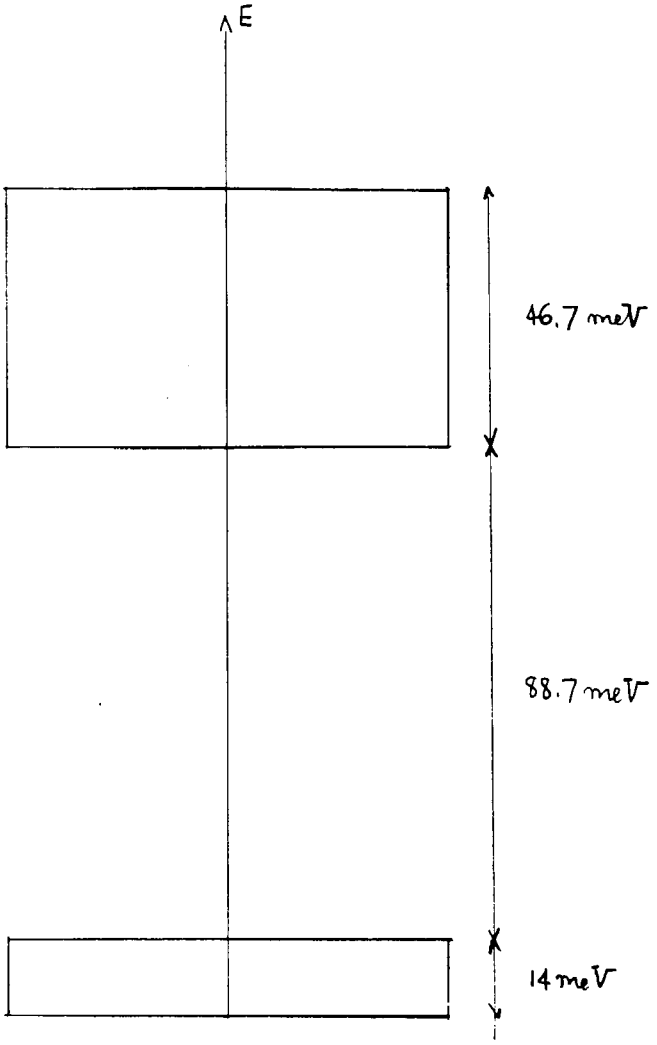

Fig 13.

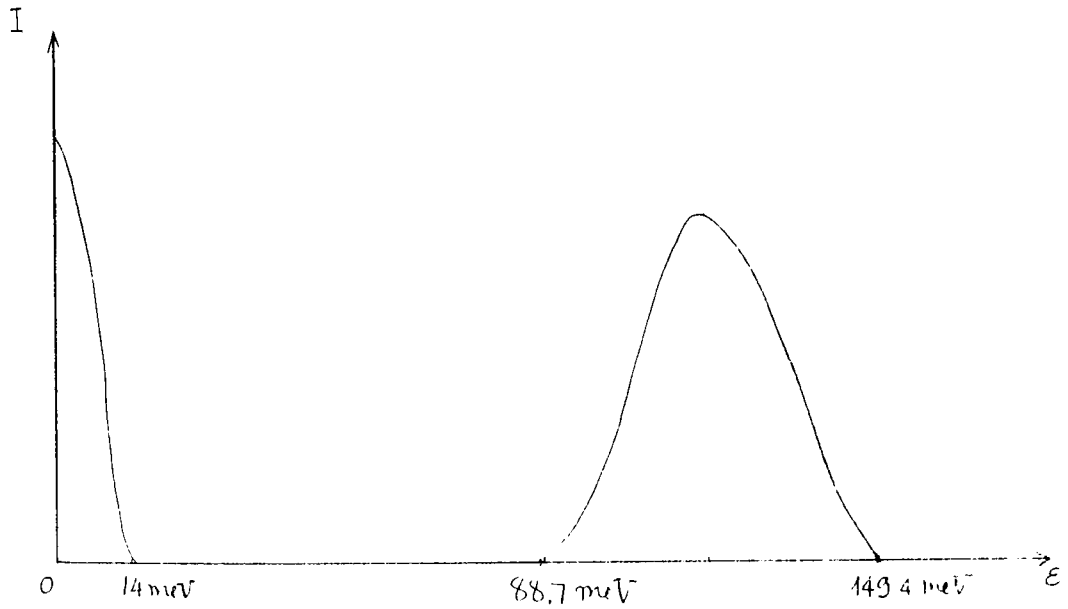

Fig 14.

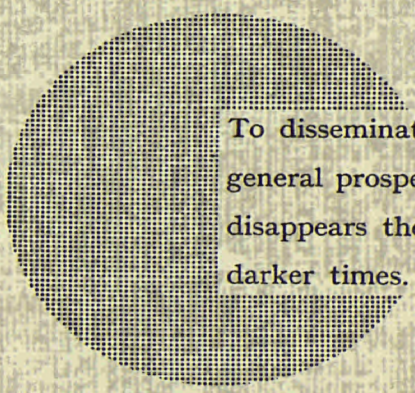

To disseminate knowledge is to disseminate prosperity — I mean general prosperity and not individual riches — and with prosperity disappears the greater part of the evil which is our heritage from darker times.

Alfred Nobel

SALES OFFICES

All Euratom reports are on sale at the offices listed below, at the prices given on the back of the cover (when ordering, specify clearly the EUR number and the title of the report, which are shown on the cover).

PRESSES ACADEMIQUES EUROPEENNES
98, Chaussée de Charleroi, Bruxelles 6

Banque de la Société Générale - Bruxelles
compte N° 964.558,

Banque Belgo Congolaise - Bruxelles
compte N° 2444.141,

Compte chèque postal - Bruxelles - N° 167.37,

Belgian American Bank and Trust Company - New York
compte No. 22.186,

Lloyds Bank (Europe) Ltd. - 10 Moorgate, London E.C.2,

Postcheckkonto - Köln - Nr. 160.861.

OFFICE CENTRAL DE VENTE DES PUBLICATIONS DES COMMUNAUTES EUROPEENNES
2, place de Metz, Luxembourg (Compte chèque postal N° 191-90)

BELGIQUE — BELGIË
MONITEUR BELGE
40-42, rue de Louvain - Bruxelles
BELGISCH STAATSBLAD
Leuvenseweg 40-42 - Brussel

DEUTSCHLAND
BUNDESANZEIGER
Postfach - Köln 1

FRANCE
SERVICE DE VENTE EN FRANCE
DES PUBLICATIONS DES
COMMUNAUTES EUROPEENNES
26, rue Desaix - Paris 15e

GRAND-DUCHE DE LUXEMBOURG
OFFICE CENTRAL DE VENTE
DES PUBLICATIONS DES
COMMUNAUTES EUROPEENNES
9, rue Goethe - Luxembourg

ITALIA
LIBRERIA DELLO STATO
Piazza G. Verdi, 10 - Roma

NEDERLAND
STAATSDRUKKERIJ
Christoffel Plantijnstraat - Den Haag

EURATOM — C.I.D.
51-53, rue Belliard
Bruxelles (Belgique)